NAVAL POSTGRADUATE SCHOOL

MONTEREY, CALIFORNIA

THESIS

COMPARISON STUDY OF LOW-LEVEL CONTROLLER TECHNIQUES FOR UNMANNED SURFACE VESSELS

by

Joseph A. Schnieders

June 2018

Thesis Advisor:	Brian S. Bingham
Second Reader:	Sean P. Kragelund

THIS PAGE INTENTIONALLY LEFT BLANK

REPORT DOCUMENTATION PAGE			*Form Approved OMB No. 0704-0188*

1. AGENCY USE ONLY *(Leave blank)*	**2. REPORT DATE** June 2018	**3. REPORT TYPE AND DATES COVERED** Master's thesis

4. TITLE AND SUBTITLE COMPARISON STUDY OF LOW-LEVEL CONTROLLER TECHNIQUES FOR UNMANNED SURFACE VESSELS	**5. FUNDING NUMBERS**
6. AUTHOR(S) Joseph A. Schnieders	
7. PERFORMING ORGANIZATION NAME(S) AND ADDRESS(ES) Naval Postgraduate School Monterey, CA 93943-5000	**8. PERFORMING ORGANIZATION REPORT NUMBER**
9. SPONSORING / MONITORING AGENCY NAME(S) AND ADDRESS(ES) N/A	**10. SPONSORING / MONITORING AGENCY REPORT NUMBER**

11. SUPPLEMENTARY NOTES The views expressed in this thesis are those of the author and do not reflect the official policy or position of the Department of Defense or the U.S. Government.

12a. DISTRIBUTION / AVAILABILITY STATEMENT Approved for public release. Distribution is unlimited.	**12b. DISTRIBUTION CODE** A

13. ABSTRACT (maximum 200 words)

Classical linear feedback control techniques are often used for low-level control of the speed and heading of an unmanned surface vessel (USV). To improve performance, two additions to generic proportional-integral-derivative are common: model-based feed-forward compensation and integration of a non-linear thrust model within the controller. This thesis contains a performance comparison of these techniques, where performance is quantified through system analysis, numerical simulation and field experiment. To investigate the impact of these different control implementations, three different scenarios are considered: speed-only, heading-only and simultaneous speed and heading control. For this particular application, feed-forward compensation results in significant performance improvement, but results in an additional control parameter that would need to be tuned to the system. The inclusion of non-linear thrust dynamics had a negligible impact on performance. Ultimately, this study suggests the performance of simple linear low-level control techniques is only modestly improved by these common model-based modifications and that this improvement may not justify the requisite additional development time.

14. SUBJECT TERMS USV, feed forward, low-level controllers, thrust model improvement, commanded compensation, non-linear thrust model	**15. NUMBER OF PAGES 107**
	16. PRICE CODE

17. SECURITY CLASSIFICATION OF REPORT	**18. SECURITY CLASSIFICATION OF THIS PAGE**	**19. SECURITY CLASSIFICATION OF ABSTRACT**	**20. LIMITATION OF ABSTRACT**
Unclassified	Unclassified	Unclassified	UU

NSN 7540-01-280-5500 Standard Form 298 (Rev. 2-89) Prescribed by ANSI Std. 239-18

THIS PAGE INTENTIONALLY LEFT BLANK

Approved for public release. Distribution is unlimited.

COMPARISON STUDY OF LOW-LEVEL CONTROLLER TECHNIQUES FOR UNMANNED SURFACE VESSELS

Joseph A. Schnieders
Lieutenant, United States Navy
BS, University of Southern California, 2011

Submitted in partial fulfillment of the
requirements for the degree of

MASTER OF SCIENCE IN MECHANICAL ENGINEERING

from the

NAVAL POSTGRADUATE SCHOOL
June 2018

Approved by: Brian S. Bingham
Advisor

Sean P. Kragelund
Second Reader

Garth V. Hobson
Chair, Department of Mechanical and Aerospace Engineering

THIS PAGE INTENTIONALLY LEFT BLANK

ABSTRACT

Classical linear feedback control techniques are often used for low-level control of the speed and heading of an unmanned surface vessel (USV). To improve performance, two additions to generic proportional-integral-derivative are common: model-based feed-forward compensation and integration of a non-linear thrust model within the controller. This thesis contains a performance comparison of these techniques, where performance is quantified through system analysis, numerical simulation and field experiment. To investigate the impact of these different control implementations, three different scenarios are considered: speed-only, heading-only and simultaneous speed and heading control. For this particular application, feed-forward compensation results in significant performance improvement but results in an additional control parameter that would need to be tuned to the system. The inclusion of non-linear thrust dynamics had a negligible impact on performance. Ultimately, this study suggests the performance of simple linear low-level control techniques is only modestly improved by these common model-based modifications and that this improvement may not justify the requisite additional development time.

THIS PAGE INTENTIONALLY LEFT BLANK

TABLE OF CONTENTS

I. INTRODUCTION....1
A. MOTIVATION....1
B. PROBLEM STATEMENT....1

II. BACKGROUND....3
A. UNMANNED SURFACE VESSEL MODEL....3
1. Introduction....3
2. Simplified Dynamic Modeling for Control....4
3. System Specification....6
B. CONTROL TECHNIQUES....8
1. Proportional-Integral-Derivative....8
2. Feed-Forward....9
3. Thruster Model Selection....11
C. RESEARCH PREDICTIONS....14
D. APPROACH....15
1. Test Cases for Comparison....15
2. Tuning Methods....16

III. SIMULATION RESULTS AND ANALYSIS....19
A. SIMULATION SETUP....19
B. MODEL VERIFICATION....21
C. DECOUPLED DYNAMICS....23
1. Heading Control....24
2. Speed Control....27
D. COUPLED DYNAMICS....43
E. SIMULATION SUMMARY....48

IV. EXPERIMENTAL RESULTS AND ANALYSIS....51
A. EXPERIMENTAL SETUP....51
1. Software and Controller Implementation....51
2. Sensor Integration and Feedback Management....52
3. Test Site Locations....53
4. Testing Apparatus and Associated Hardware....55
5. Environmental Considerations....58
B. EXPERIMENTAL TESTING APPROACH....59
C. DECOUPLED DYNAMICS....59
1. Heading Control....60

2. Speed Control 63
D. COUPLED DYNAMICS 72
E. EXPERIMENTAL SUMMARY 77

V. CONCLUSIONS 79
A. COMPARISON OF SIMULATION AND EXPERIMENT RESULTS 80
B. CONTROLLER TECHNIQUE BENEFITS ANALYSIS 81
C. FUTURE WORK 82

LIST OF REFERENCES 83

INITIAL DISTRIBUTION LIST 87

LIST OF FIGURES

Figure 1. Step Response of a Generic Second Order System and Performance Characteristics. Source: [11]. 2

Figure 2. 6 DOF Coordinate Frame. Adapted from [14]. 3

Figure 3. CLEARPATH Robotics™ KINGFISHER. Source: [14]. 7

Figure 4. Generalized PID Feedback Loop. Adapted from [18]. 9

Figure 5. Generalized Command-Compensated Control Loop. Source: [20] 10

Figure 6. Simplified Feed-Forward Control Model for USV 11

Figure 7. Linear Thrust Command Relation. 13

Figure 8. Non-Linear Thrust Command Relation. Source: [16] 13

Figure 9. Complete Simulation Model—Top Layer 20

Figure 10. PID Controller—Sub-Layer 20

Figure 11. USV Simulation Model—Sub-Layer 21

Figure 12. USV Equations of Motion—Sub-Layer 21

Figure 13. Open-Loop USV Model 23

Figure 14. Model Verification Results 23

Figure 15. Tuning Step Responses—Heading Control—Linear Thrust Model Approximation 24

Figure 16. Tuning Step Responses—Heading Control—Non-Linear Thrust Model Approximation 25

Figure 17. Heading Control—Optimized Step Response—Linear and Non-Linear Thrust Model Approximations 27

Figure 18. Tuning Step Responses—Low-Speed—Linear Thrust Model Approximation 29

Figure 19. Tuning Step-Responses—Low Speed Control—Non-Linear Thrust Model Approximation 29

Figure 20. Optimized Step Responses—Low-Speed Control—Linear and Non-Linear Thrust Model Approximations 31

Figure 21. Speed Control with Feed-Forward Architecture in Simulink Model....32

Figure 22. Tuning Step Responses—Low-Speed Control without Feed-Forward Compensation 33

Figure 23. Tuning Step Responses—Low-Speed Control with Feed-Forward Compensation 34

Figure 24. Optimized Step Response—Low-Speed Control—Feed Forward Control 35

Figure 25. Optimized System Response—Feed-Forward Compensation—Integrator Effort Comparison....36

Figure 26. Tuning Step Responses—High-Speed—Linear Thrust Model Approximation 37

Figure 27. Tuning Step-Responses—High Speed Control—Non-Linear Thrust Model Approximation....37

Figure 28. Tuning Step-Response—High-Speed Control—Second Gain Testing Iteration 38

Figure 29. Optimized Step-Response—High-Speed—Linear and Non-Linear Thrust Model Approximations....39

Figure 30. Tuning Step Responses—High-Speed Control without Feed-Forward Compensation 41

Figure 31. Tuning Step Responses—High-Speed Control with Feed-Forward Compensation 41

Figure 32. Optimized Step Response—High-Speed Control—Feed Forward Control 42

Figure 33. Optimized System Response—Feed-Forward Compensation—Integrator Effort Comparison....43

Figure 34. Coupled Dynamics System Responses—Low Speed Turn 44

Figure 35. Low Speed Turn—Integrator Effort Comparison....45

Figure 36. Dynamics System Responses—High Speed Turn 47

Figure 37. High Speed Turn—Integrator Effort Comparison 48

Figure 38. Simulink Model of Controller with ROS Functionality 52

Figure 39. CAVR Test Tank 54

Figure 40. Lake El Estero, Monterey, California. Adapted from [26]. 55

Figure 41. Symbolic Representation of Testing Information Exchange 56

Figure 42. Lake El Estero Experimental Setup Overview 57

Figure 43. Lenonvo ThinkPad T460 with Logitech F310 Gamepad USB Controller. 57

Figure 44. CLEARPATH Wireless Router and Tripod. 58

Figure 45. Experimental Heading Control—Oscillation Error Example 61

Figure 46. Heading Control—Experimental Step Responses—Linear and Non-Linear Thrust Model Approximations 62

Figure 47. Optimized Experimental Step Responses—Low Speed Control – Linear and Non Linear Thrust Model Approximations 65

Figure 48. Optimized Step Response—Low-Speed Control—Feed Forward Control 67

Figure 49. Optimized System Response—Feed-Forward Compensation—Integrator Effort Comparison.....67

Figure 50. Optimized Experimental Step Responses—High Speed Control – Linear and Non Linear Thrust Model Approximations 69

Figure 51. Optimized Step Response—High Speed Control—Feed Forward Control 71

Figure 52. Optimized Experimental Step Responses—High Speed Control—Feed Forward Control Integrator Analysis 71

Figure 53. Optimized System Response—Feed-Forward Compensation—Integrator Effort Comparison.....72

Figure 54. Optimized Experimental System Responses—Low Speed Turn—Coupled Dynamics.....73

Figure 55. Optimized Experimental System Response—Low Speed Turn—Compensation—Integrator Effort Comparison.....75

Figure 56. Optimized Experimental System Responses—Low Speed Turn—Coupled Dynamics.....76

Figure 57. Optimized Experimental System Response—Low Speed Turn—Compensation—Integrator Effort Comparison.....77

LIST OF TABLES

Table 1. Model Assumptions and Justifications 6

Table 2. KF-USV System Specification 7

Table 3. Motor Command to Thruster Force Relationship 12

Table 4. Test Case Definition Matrix 16

Table 5. Gain Constant Testing Values 17

Table 6. Model Verification Results 22

Table 7. Heading Control—Linear and Non Linear Thrust Model Approximation—Step Response Characteristic Comparison 26

Table 8. Heading Control—Optimized Controller—Step Response Characteristic Comparison 27

Table 9. Performance Characteristic Comparison—Low-Speed Control—Linear and Non Linear Thrust Model Approximation 30

Table 10. Optimized Performance Characteristics Comparison—Low-Speed Control—Linear and Non-Linear Thrust Model Approximations 31

Table 11. Performance Characteristics Comparison—Low-Speed Control—Feed Forward Compensation 33

Table 12. Optimized Performance Characteristics—Low-Speed Control—Feed-Forward Compensation 34

Table 13. High Speed Control—Refined Tuning Gain Table 38

Table 14. Optimized Performance Characteristics—High Speed—Linear and Non-Linear Thrust Model Approximations 39

Table 15. Optimized Performance Characteristics—Low-Speed Control—Feed-Forward Compensation 42

Table 16. Coupled Dynamics—Low Speed Turn—Performance Characteristics Comparison—Heading Response 45

Table 17. High Speed Turn—Performance Characteristics Comparison—Heading Response 47

Table 18. ROS Nodes, Topics and Messages of Interest for Research.....53

Table 19. Selected Weather Data from Experimental Testing Days. Source: [27].....59

Table 20. Heading Control—Experimental Results—Performance Characteristics.....62

Table 21. Optimized Experimental Performance Characteristics Comparison—Low-Speed Control—Linear and Non-Linear Thrust Model Approximations.....65

Table 22. Optimized Experimental Performance Characteristics—Low-Speed Control—Feed-Forward Compensation.....66

Table 23. Optimized Experimental Performance Characteristics Comparison—High-Speed Control—Linear and Non-Linear Thrust Model Approximations.....69

Table 24. Optimized Experimental Performance Characteristics—High-Speed Control—Feed-Forward Compensation.....70

Table 25. Optimized Experimental Performance Characteristics Comparison—Coupled Dynamics—Heading Response at Low Speed.....74

Table 26. Optimized Experimental Performance Characteristics Comparison—Coupled Dynamics—Heading Response at Low Speed.....76

LIST OF ACRONYMS AND ABBREVIATIONS

ASW	Anti-Submarine Warfare
CAVR	Center for Autonomous Vehicle Research
CUSV	Common Unmanned Surface Vessel
DOF	Degrees of Freedom
EOM	Equations of Motion
INS	Inertial Navigation System
KF-USV	KINGFISHER USV
MDUSV	Medium Displacement Unmanned Surface Vehicle
MIW	Mine-Warfare
MRAC	Model Reference Adaptive Control
OEM	Original Equipment Manufacturer
PD	Proportional-Derivative
PI	Proportional-Integral
PID	Proportional-Integral-Derivative
ROS	Robot Operating Software
SNAME	Society of Naval Architects and Marine Engineers
USN	United States Navy
USV	Unmanned Surface Vessel
X-USV	*X-class* Unmanned Surface Vessel

THIS PAGE INTENTIONALLY LEFT BLANK

ACKNOWLEDGMENTS

First, I would like to express my eternal gratitude to my wife, Sirena. I am indebted to you for all the love, encouragement and patience you provided me while writing this thesis. I could not have done it without you. Thank you.

I would also like to thank my children for being a source of inspiration and reservoir of energy. You reminded me every day that a love for learning new things is inherent and infectious.

I would like to thank my parents, Bill and Colleen, for their support, love and guidance through the years. You never relented in pushing me to recognize and pursue achieving my potential in life.

I would like to thank my second reader, Dr. Sean Kragelund, for providing guidance during experimentation and valuable comments and inputs into this thesis.

Lastly, a deep and sincere thank you to Dr. Brian Bingham for all the guidance, wisdom, and patience you displayed. Completing this thesis under your advisory has been one of the most rewarding experiences in my life and it would not have been possible without you.

THIS PAGE INTENTIONALLY LEFT BLANK

I. INTRODUCTION

A. MOTIVATION

The United States Navy (USN) is pursuing the employment of unmanned surface vessels (USV) to accomplish resource-intensive, long-endurance and meticulous tasks that have been historically fulfilled by manned vessels. The desired tasks are often related to missions categorized into anti-submarine warfare (ASW) and mine warfare (MIW). This includes leveraging the Defense Advance Research Project Agency's (DARPA) medium-displacement unmanned surface vehicle (MDUSV) *Sea Hunter* to actively track submarines through vast waterspace [1] and utilizing a Common USV (CUSV) to pull minesweeping equipment through potential mined waterways [2]. These are examples of large-scale USVs but more pertinent to the following research is the Navy's pursuance of X-class USVs (X-USV), which are characterized as less than 3.048 meters (10 feet) and designed to fulfill missions where "stealth, modularity, expendability, light weight, and low cost are critical" [3]. Inherent to all these applicants is the need for control systems to conduct functions in the absence of manned crews. The MDUSV, CUSV, and X-USV each require low-level controllers for heading and speed execution to fulfill higher-level functions such as submarine tracking or mine hunting. The effectiveness in the response of these low-level controllers can be critical to the overall mission accomplishment since they impact a USV's ability to carefully navigate hazardous waters, avoid navigational hazards, and/or maintain a desired track.

B. PROBLEM STATEMENT

Many different control techniques can and have been applied to a small-scale USV to maintain its heading and speed [4]-[9]. These include but are not limited to Proportional-Integral-Derivative (PID) controllers [5], PID with augmentations such as a feed-forward [9], gain-scheduling [10], and adaptive controllers (e.g., L1 and model reference adaptive control [MRAC]) [6], [7]. Controller selection depends on the degree of desired performance (i.e., accuracy and reliability) and can have constraints on computational resources, sensor integration, and previous knowledge of the system or model required for

implementation. They also vary in the amount of tuning required to produce effective results. All of these factors can enable or inhibit control selection.

This research aims to objectively and subjectively compare and contrast benefits and drawbacks to a limited combination of control techniques with regards to effectiveness and tuning requirements. We will utilize step response metrics such as rise time (T_r), settling time (T_s), percent overshoot, and steady state error (see Figure 1 for an example) generated from set point changes in speed and heading. This is then compared to predicted changes and also evaluated for consistency. In addition to the analytical comparison, there will be discussion in the differences required to tune the controllers and ultimately recommendations made in further studies.

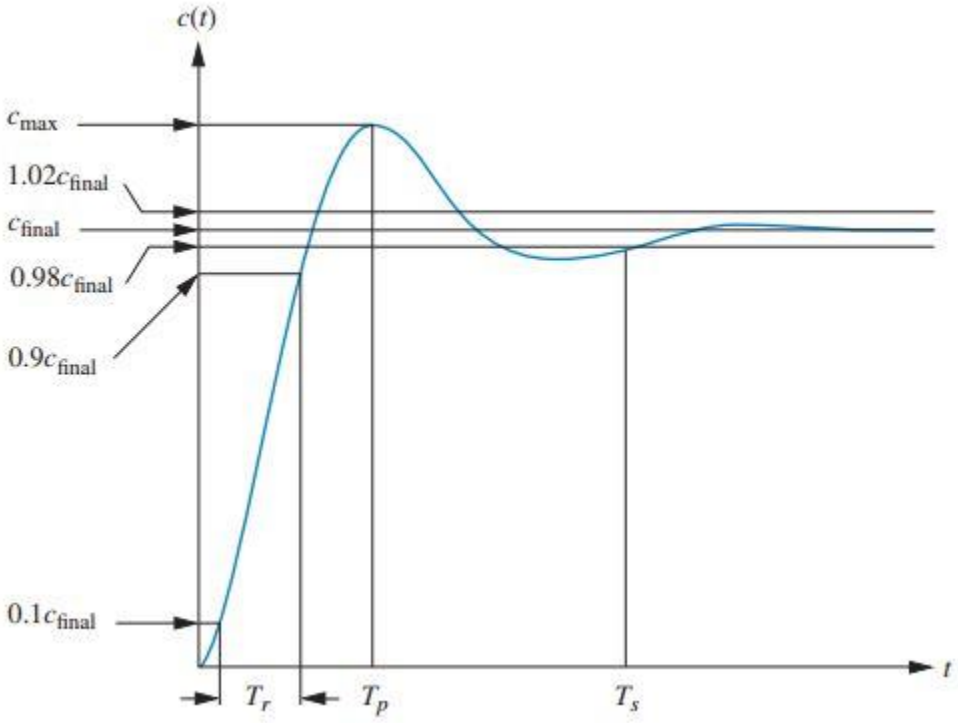

Figure 1. Step Response of a Generic Second Order System and Performance Characteristics. Source: [11].

II. BACKGROUND

A. UNMANNED SURFACE VESSEL MODEL

1. Introduction

Fossen [12], [13], describes the dynamics of a marine vessel as a general six degrees of freedom (DOF) rigid-body relative to an inertial based coordinate frame. Figure 2 provides the basis for coordinate frame and direction discussion during further analysis.

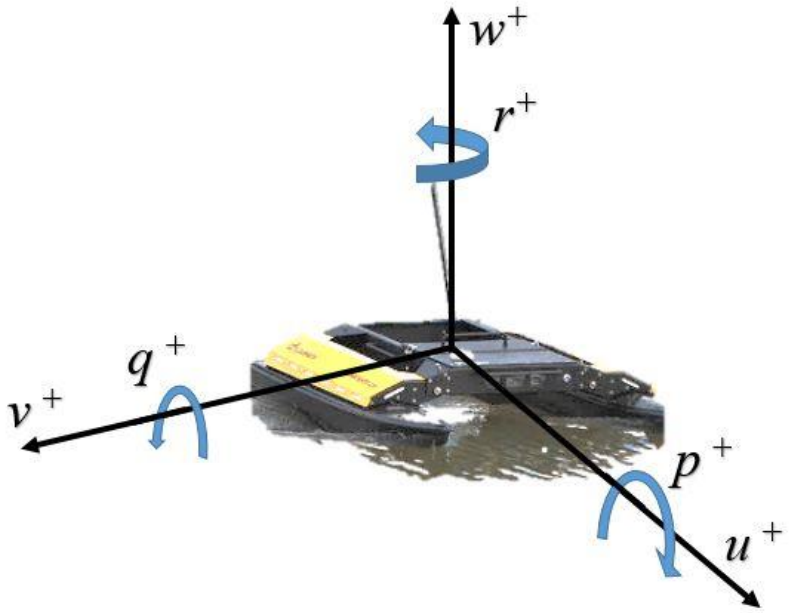

Figure 2. 6 DOF Coordinate Frame. Adapted from [14].

These six DOF can be mathematically reduced to a matrix-vector equation [13] utilizing the Society of Naval Architects and Marine Engineers' (SNAME) notation [15] and expressed as

$$M_{RB}\dot{\upsilon}+C_{RB}(\upsilon)\upsilon+D(\upsilon)\upsilon+g(\eta)+g_0=\tau_{RB}+\tau_{wave}+\tau_{wind}$$
$$\upsilon=[u,v,w,p,q,r]^T,\ \eta=[x,y,z,\phi,\theta,\psi]^T,\ \tau_{RB}=[X,Y,Z,K,M,N]^T \quad (1)$$

where,

- M_{RB} is the mass-inertia matrix
- $C_{RB}()$ is the Coriolis and centripetal matrix
- $D()$ is the damping matrix
- $g()$ is a generalized gravitational and buoyancy force vector
- g_o is a collection of static, ballast and restoring forces and moments
- τ_{wave} and τ_{wind} are wind and wave external forces and moments acting on the rigid body
- u, v, and w are the surge, sway and heave linear velocities respectively
- p, q, and r are the roll, pitch and yaw angular velocities respectively
- x, y, and z are positions of the body as related to the center of gravity
- ϕ, θ, and ψ are Euler angles with respect to the coordinate frame of choice
- X, Y, Z, K, M, and N are the external moments and forces

For this research we will be designing and implementing controllers for forward speed (surge, u) and heading (yaw, ψ).

2. Simplified Dynamic Modeling for Control

It is beneficial to simplify and resolve the resulting equations of motion of the aforementioned generalized six DOF model in order to begin implementing simple control techniques. First, speed and heading (i.e., by steering) equations are defined as

$$M_{RB}\dot{u} - M_{RB}x_g r^2 - M_{RB}vr = X_{\dot{u}}\dot{u}_r + Y_{\dot{v}}v_r r + Y_{\dot{r}}r^2 + X_u u + X_{u|u|}u|u| + \tau \quad (2)$$

$$I_z\dot{r} + M_{RB}x_g\dot{v} + M_{RB}x_g ru - Y_{\dot{r}}\dot{v} - N_{\dot{r}}\dot{r} - Y_{\dot{v}}v_r u + X_{\dot{u}}u_r v - Y_{\dot{r}}ru - N_v v + N_{v|v|}v|v| + N_r r + N_{r|r|}r|r| = \tau \quad (3)$$

respectively [13], [16]. These equations include effects of inertia, Coriolis, added-mass, linear and quadratic drag, coupled drag, and Monk moments. They also assume that the

vessel generates thrust in the surge direction via a propeller or thruster and utilizes a rudder or other control surface for steering. The USV utilized for this research has independent non-rotating port and starboard water jets that provide thrust and steering. By combining aspects from models of Fossen [12], [13] , Caccia, Veruggio et al., [10], [12], [13] and making the assumptions listed in Table 1, we arrive at two simplified and decoupled equations for thrust and steering,

$$M_{RB}\dot{u} + X_{|u|u}|u|u + X_u u = X_c \tag{4}$$

$$I_z\ddot{\psi} + \left(N_r + N_{r|r|}|\dot{\psi}|\right)\dot{\psi} = N_c \tag{5}$$

where

- $X_{|u|u}|u|u$ and $X_u u$ represent the quadratic and linear drag associated with the surge direction and $N_r + N_{r|r|}|\dot{\psi}|$ is the linear drag associated with turning.
- X_c is the total control force (i.e., thrust) in the surge direction
- I_z is the moment of inertia about vertical axis with respect to the center of gravity
- N_c is the total control torque about the vertical axis.

Table 1. Model Assumptions and Justifications

Assumption	Justification
Uncoupled Dynamics (surge/yaw)	For simplicity of control design.
Sway (±*v*) motion is neglected	Sway motion (i.e., side-slip) not observable through previous experiments with particular USV [16].
Added mass, $X_{\dot{u}}$, is neglected.	Caccia et al. [10] stated for a small catamaran vessel that this value is typically less than 5% of the vessel's mass and therefore negligible.
Centripetal terms, $M_{RB}x_g r^2$ & $Y_{\dot{r}}r^2$, terms are neglected.	Caccia et al. [10] stated for turning rates of less than 10 degrees/second is negligible.

Neglecting the coupled dynamics allows each degree of freedom to be modeled as single-input single-output (SISO) systems with individual controllers. However, this is a simplification that ignores experimental research that indicates there is strong coupling of heading and surge through drag, Coriolis terms and other dynamics for small USVs with catamaran hull forms and water jets [17].

3. System Specification

The vessel used for this research is a CLEARPATH Robotics™ KINGFISHER USV (KF-USV). The KF-USV is pictured in Figure 3. It is a catamaran hull form with two non-directional water jets utilized for thrust and steering. Based on testing by Manzini [16], Table 2 displays the system specifications and physical parameters of concern to our dynamic model.

Figure 3. CLEARPATH Robotics™ KINGFISHER. Source: [14].

Table 2. KF-USV System Specification

Specification	**Value**
Mass (M_{RB})	36.0 kg Payload included
Moment of Inertia (I_z)	6.25 $kg \bullet m^2$ Based on thin-disk assumption
Quadratic surge drag ($X_{\|u\|u}$)	16.9 $N/(m/s)^2$ Determined experimentally
Linear surge drag (X_u)	0.0 $N/(m \bullet s)$ Determined experimentally
Quadratic yaw drag ($N_{r\|r\|}$)	139.0 $(N \bullet m)/(rad/s)^2$ Determined experimentally
Linear yaw drag (N_r)	0.0 $N/(rad/s)$ Determined experimentally

B. CONTROL TECHNIQUES

1. Proportional-Integral-Derivative

One of the most fundamental and common techniques of feedback control is the use of a Proportional-Integral-Derivative (PID) controller. Figure 4 displays a general visualized feedback loop with a PID controller operating on the error, *e*, between the output, *y*, and the desired set-point, y_{sp}. Inherent to a PID controller are the three components or terms that operate on the error in different ways. The proportional terms operate as a multiplicative factor on the error. The integral term evaluates the error as a function of time and drives the steady state error between the output and set point to zero. The derivative term operates on the rate change of the error and can help in minimizing factors such as overshoot and/or oscillation. Åstrom [18] provides three common mathematical definitions of a PID controller,

$$u(t) = K\left(e(t) + \frac{1}{T_i}\int_0^t e(\tau)d\tau + T_d\frac{de(t)}{dt} \right) \tag{6}$$

$$G(s) = K\left(1 + \frac{1}{sT_i} + sT_d \right) \tag{7}$$

$$G(s) = K_P + \frac{K_i}{s} + sK_d\,. \tag{8}$$

Equations (6) and (7) are the textbook representations with a single gain, *K*, in the time and "s" domain respectively. Equation (8) is the form that, when implemented, a controller most closely represents with respect to *tuning*. This is because K_P, K_i, and K_d are the gains associated with the proportional, integral, and derivative terms respectively and are the proverbial *knobs* referenced when one talks about *turning the knobs* for controller tuning. The selection of these gain values are the primary consideration when comparing different tuning techniques and requirements.

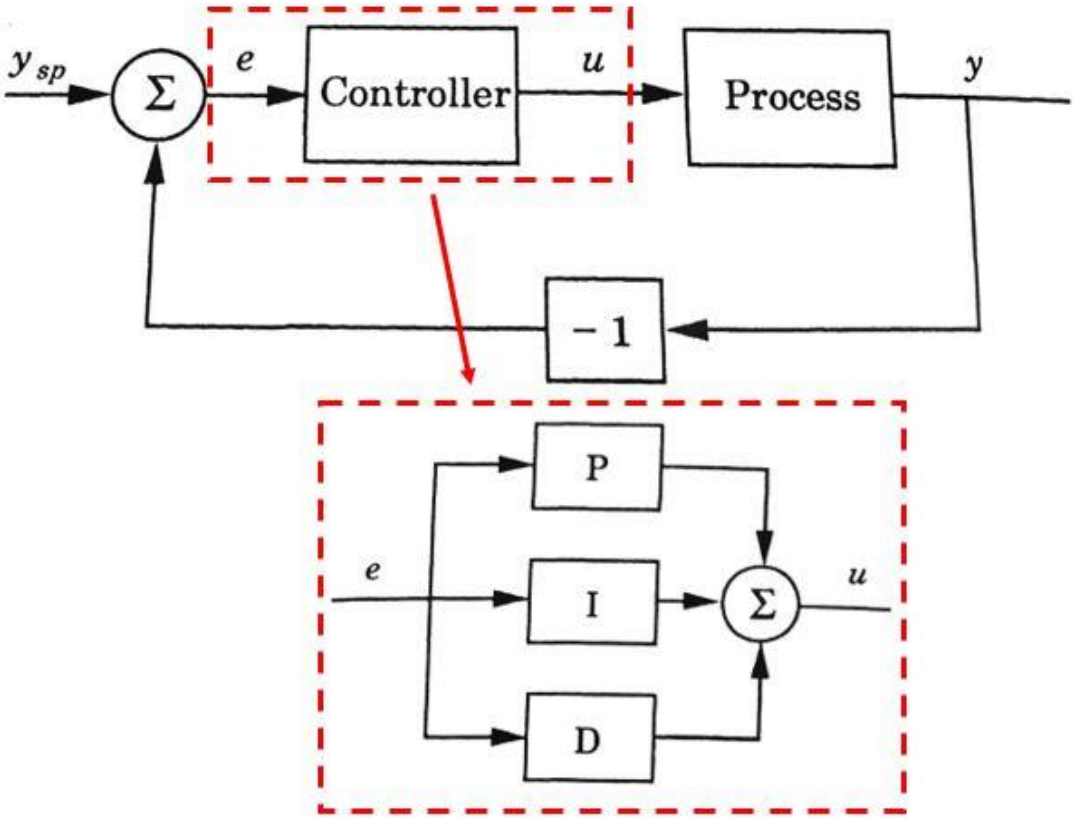

Figure 4. Generalized PID Feedback Loop. Adapted from [18].

2. Feed-Forward

A phenomena associated with PID controllers is the effect of integral *wind-up*. Wind-up is caused when the integral term's effect grows too large due to the accumulation of error over time. When the integral term is too large, the controller can fail to respond fast enough to changing dynamics, which can be undesired for certain applications. One of the common techniques to counter this is the use of a feed-forward term in the control process. This term leverages knowledge about the system (e.g., model dynamics or system disturbances) and provides that value associated with a set point early in the control process [19]. As it relates to the integral term, one of the research questions for this thesis is: Will an adequate feed-forward term minimize the effect of the integrator on the overall system?

Doebelin [20] proposes that there are two common techniques of feed-forward control: disturbance-compensated control and command-compensated control. Disturbance

control is based on having a sensor able to detect and measure a disturbance and then deducing its mathematical relationship to the system's input. The solution of this empirical relationship can be subtracted from the reference input in an open-loop configuration to improve response. Command-compensated control is the concept of utilizing the relationship between a system's desired set-point and its expected output, based on empirical knowledge of the system. A generalized command-compensated control from [20] is shown in Figure 5 where *V* and *C* represent input and output, G_C is the command-compensated term, and G_{11}, G_2 and *H* represent general transfer function terms in the control loop.

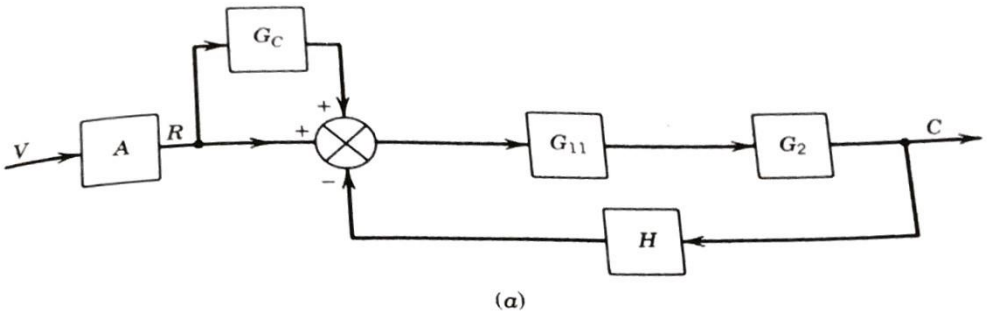

Figure 5. Generalized Command-Compensated Control Loop. Source: [20]

We will consider only command-compensated control and refer to it exclusively as feed-forward control. For this research, we utilized this concept as it applied to speed control because of the dynamics of the surge model. Assuming the simplified model from (4), we can estimate the force required at a desired speed. It is not mathematically analogous for heading because there is not a steady state force that is required to complete a certain change in direction. Figure 6 is a simplified illustration on the feed-forward control that is incorporated for this research.

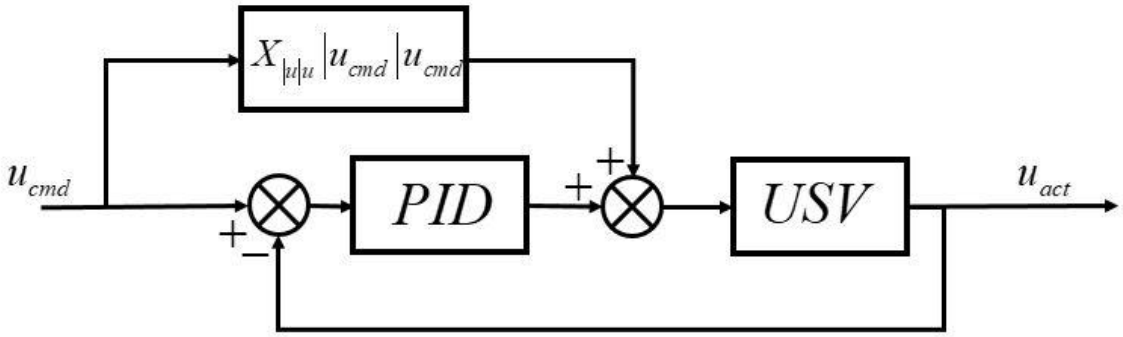

Figure 6. Simplified Feed-Forward Control Model for USV

3. Thruster Model Selection

The last control technique that this research addresses is the selection of a relationship between thruster force and motor command to the USV. Feedback control with a PID controller assumes the plant has linear properties which is inaccurate based on our model of the system from (4)-(5). Therefore, we can utilize a non-linear thrust model to linearize the system around a set of known data points in order to improve the controller's efforts. This is done relating the thruster output and motor control commands. We know that the command to each electrical motor on the USV is received as a signal in the range of -1 to 1 where -1.0 is full reverse and +1.0 is full forward. The commanded input and sensors providing feedback information do so in physical terms (e.g., physical position, velocity, angle, etc.). Therefore, the controller is assumed to output thrust requirements in force [N] and thus, needs to be converted to a signal of meaning for the motor. This research will treat this relationship as either linear or a non-linear approximation. This research only contends with the forward direction and therefore the linear relationship assumes that the motor command for one thruster from [0 to 1] varies from [0 to 20.7] [N] where 20.7 [N] represents half the maximum force of two thrusters operating at steady-state. An assumed linear relationship between these variables, where the max forward and reverse commands, -1.0 and +1.0, are equal to 20.7 [N] for one thruster (i.e., 41.4 [N] for two thrusters) is presented in Figure 7. This model is the linear thrust model approximation. The non-linear relationship is based on testing of the KF-USV conducted by Manzini and is tabulated in Table 3 and displayed graphically in Figure 8.

The basis of this control technique is founded in similar testing and theory of thruster model accuracy comparison in marine vessels by Whitcomb, Smallwood, et al., in [21]–[23]. They conducted extensive research into the effects of improving thruster model accuracy for control improvement. Their research found that improving model accuracy has obvious benefits, although it is dependent upon the validity of the physical parameters that are implemented. Whitcomb concluded that model-based solutions compared preferably to standard feedback control approximations in control over a wide-range of testing set points and also responded much better to transients [22], [23]. Conversely, Smallwood concluded that a non-linear approximation similar to what this research investigates can improve control and steady-state response. However, if this approximation is based on inaccurate information, this approach can degrade performance more severely than a simple linear approximation with similar errors [21]. Both Whitcomb and Smallwood address the effect that thrust saturation has on the thrust model and system performance. Thrust saturation occurs when a controller places infinite demand on a thruster, but physical constraints of the motor saturate or limit the output possible. Thruster saturation can visually be seen in Figure 8 over the last ~30% of the curve where the response ceases to change despite greater commanded input. This is a non-linearity of the physical response that affects the system at peak commanded inputs and is a focus of this research, since we expect the non-linear approximation to improve the response.

This research will seek to determine if the thrust model curve improves the performance over the full spectrum of testing or only in specific cases, and whether it has detrimental effects in other cases.

Table 3. Motor Command to Thruster Force Relationship

Motor Command [-]	0.0	0.1	0.2	0.3	0.4	0.5	0.6	0.7	0.8	0.9	1.0
Thruster Force [N]	0.0	0.3	1.1	4.1	7.4	10.5	14.4	19.7	20.6	20.65	20.7

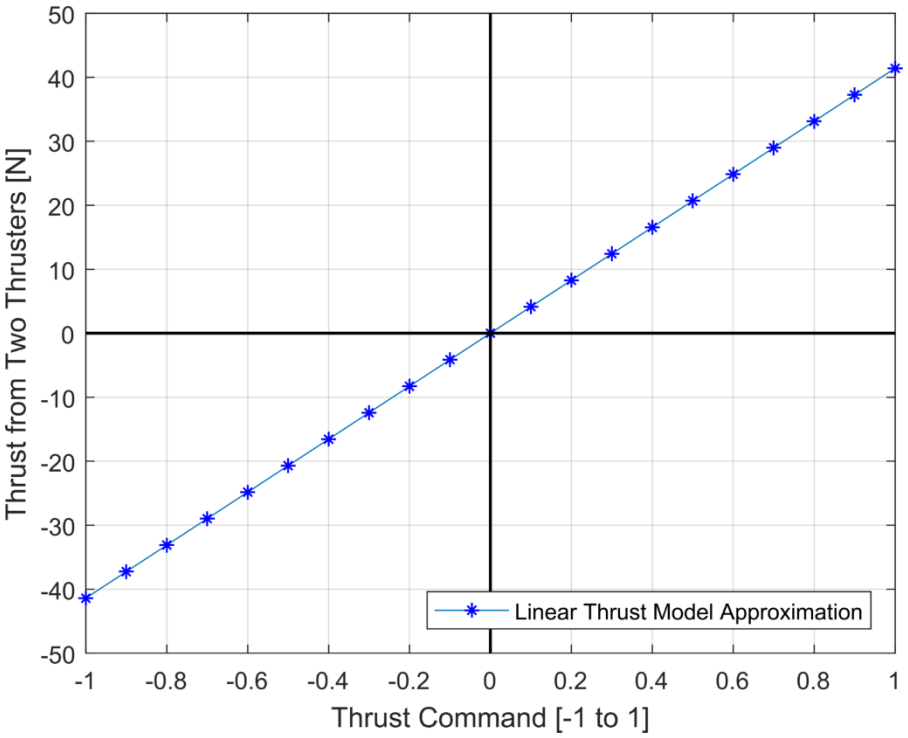

Figure 7. Linear Thrust Command Relation.

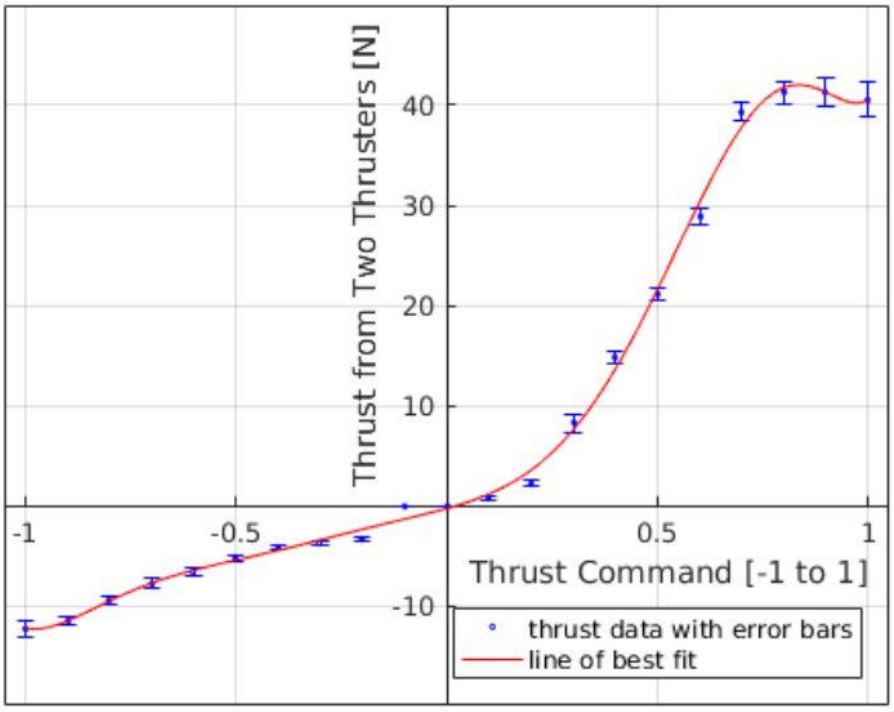

Figure 8. Non-Linear Thrust Command Relation. Source: [16]

C. RESEARCH PREDICTIONS

Questions and predictions of this study have been stated or alluded to in the previous discussion. The following is a formalization of these items that will be continually referenced in the analysis and conclusions of following sections. These items have effects on later decisions (e.g., choosing to test linear and non-linear thrust models for same magnitude gains across the speed spectrum) in order to compare to theory.

Predictions:

1. The non-linear thrust model approximation will perform with greater performance consistency with the same tuning (i.e., identical magnitude of gains) across low and high speed regions than the linear thrust model approximation. This assumes that the non-linear thrust model dynamically responds to the system more consistently at these extremes because it more closely resembles the physics of the real-world thruster response.

2. The non-linear thrust model approximation will provide improved heading control response because turning to a precise heading will require the system to respond, during transients, at high and low speeds for an accurate response.

3. Feed forward compensation will reduce the effort/effect caused by the integrator of the PID controller and will reduce integrator wind-up for speed control. This assumes that utilizing experimental speed and thruster mapping will allow the system to respond more aggressively to speed changes. This will therefore require less steady-state error resolution and error to integrate.

4. Feed forward compensation will improve baseline performance of surge response with no-tuning due to the same factors as stated in the previous prediction.

D. APPROACH

The chronological order of testing was to conduct simulation-based testing to arrive at numerical solutions and then compare them to experimental real-life results with the USV. The simulation testing consisted of a process of incremental controller design and model dynamics. The controllers and techniques that resulted from simulation were incorporated into the experiments, and then the overall trends and results were compared and analyzed.

1. Test Cases for Comparison

The goal of this research is to test and evaluate the effectiveness of each of the control techniques individually and in combination. These test cases are important because they relate well to real world applications; testing at low-speeds supports in understanding the dynamics as they may relate to station-keeping or surveying operations, while high-speed testing is representative of vessel or marine-life tracking. The following defines the variables and their range of testing:

- **Speed Control:**
  - Yes—High Speed (HS) or Low Speed (LS). Defined as $1.25-1.50\left[m/s\right]$ and $0.00-0.25\left[m/s\right]$ step input respectively.
  - No (NS).
- **Heading Control:** Yes (HH) or No (NH). Yes defined as $0-45\left[\deg\right]$ step input.
- **Feed-Forward:** Yes (FF) or No (NF).
- **Thrust Model:** Nonlinear (NL) or Linear (LL).

Table 4 displays a simplified matrix identifying the test cases under consideration for this research

Table 4. Test Case Definition Matrix

Speed and Heading Control	Feed-Forward (FF/NF)	Thrust Model (LL/NL)	Number of Cases (Tested/ Possible)
Decoupled: Low Speed Constant Heading	Tested for both cases	Tested for both cases	4/4
Decoupled: High Speed Constant Heading	Tested for both cases	Tested for both cases	4/4
Decoupled: No Speed 45 Deg Change	Not tested	Tested for both cases	2/4
Coupled: Low Speed 45 Deg Course	Tested for both cases	Tested for both cases	4/4
Coupled: High Speed 45 Deg Course	Tested for both cases	Tested for both cases	4/4

2. Tuning Methods

A tenant of this research is the comparison of tuning requirements for different controller designs. It is an inherent and most often user-dependent property of implementing feedback control. This means that although a certain control technique may be the proper choice for a given system, it may still perform poorly if it is tuned improperly. A difficulty of this research is developing a robust method to determine the difficulty of tuning. Ultimately the comparison between techniques is usually highly subjective. The following methods were used during this research to maintain objectivity.

a. Testing Against Common Gains

In lieu of utilizing a tuning algorithm such as Ziegler-Nichols, all simulation test cases that are generalized in Table 4 were tested against a similar set of gain constants, K_P, K_i, and K_d as is consistent with a PID controller described by Equation (8). These gains were varied to test the sensitivity of each test case to the changes in the proportional, integral and derivative gains, first individually, and then combined in different proportions. As a result, each simulation test case was evaluated for a minimum of 13 trials (see Table 5). Next, each controller was individually tuned based on the 13 simulated responses, thus

providing a basis of objective comparison for controller tuning. This large number of trials could not be feasibly implemented during the experimental testing, but it provides a basis for further research.

Table 5. Gain Constant Testing Values

Test #	K_P	K_i	K_d
1	1	0	0
2	10	0	0
3	100	0	0
4	1	1	0
5	1	0.01	0
6	1	0.1	0
7	1	10	0
8	1	100	0
9	1	0	1
10	1	0	0.01
11	1	0	0.1
12	1	0	10
13	1	0	100

THIS PAGE INTENTIONALLY LEFT BLANK

III. SIMULATION RESULTS AND ANALYSIS

A. SIMULATION SETUP

Simulation was conducted in order to test and evaluate the mathematical representation of our feedback control system and utilize the numerical results as a basis of comparison for future experimental testing. The mathematical representation of our system consists of the models for surge (4) and yaw (5), the PID controller (8), a varying relationship between linear and non-linear thrust approximations, and the possible inclusion of a command-compensated algebraic relationship. For example, one iteration of a numerical result would feed the error signal (i.e., difference between current output and user-defined set point) into a PID controller with user-defined gains (e.g., K_P, K_I, and K_D). This output of the PID controller would be converted into a motor control signal, feeding the vehicle model, which converts the signal into a thruster force which produces a forward velocity and yaw rate which integrated over the simulation time would result in a heading. This result would then be fed back to for comparison to the set-point, calculated as the error.

In order to obtain useful information on the performance of these controllers, it is required that this process is numerically iterated or simulated. MATLAB and Simulink were used to conduct the simulation-based testing design based on their graphic user interface and visualization capabilities. MATLAB was utilized for iteration scripting, analyses, plotting and exporting simulation data. Simulink was the model-based framework for building the control process and conducting the tests. Figures 9–12 represent portions and examples of the graphic representation Simulink provides for simulation testing. Figure 9 is the top-layer and visualizes how a commanded value (left-most graphics) can be processed through the PID controllers, converted into thruster command signals, to drive the plant model, whose outputs are plotted, saved to the MATLAB workspace, and returned to calculate error. Figures 10–12 show the visual representation of the PID controller, thrust force vectoring, and an example of the EOM modeling, respectively.

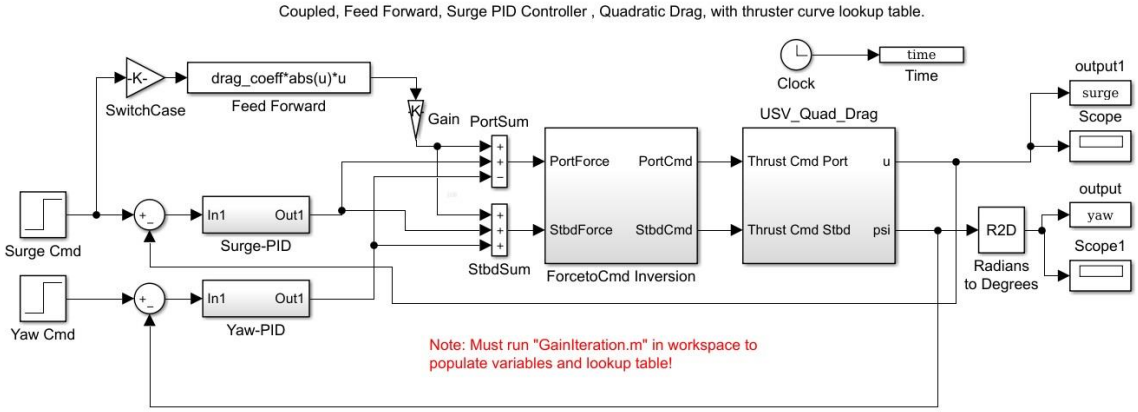

Figure 9. Complete Simulation Model—Top Layer

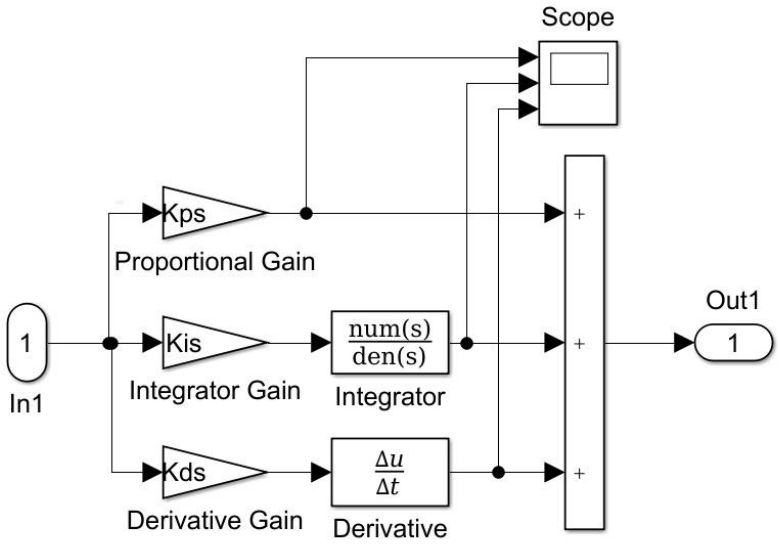

Figure 10. PID Controller—Sub-Layer

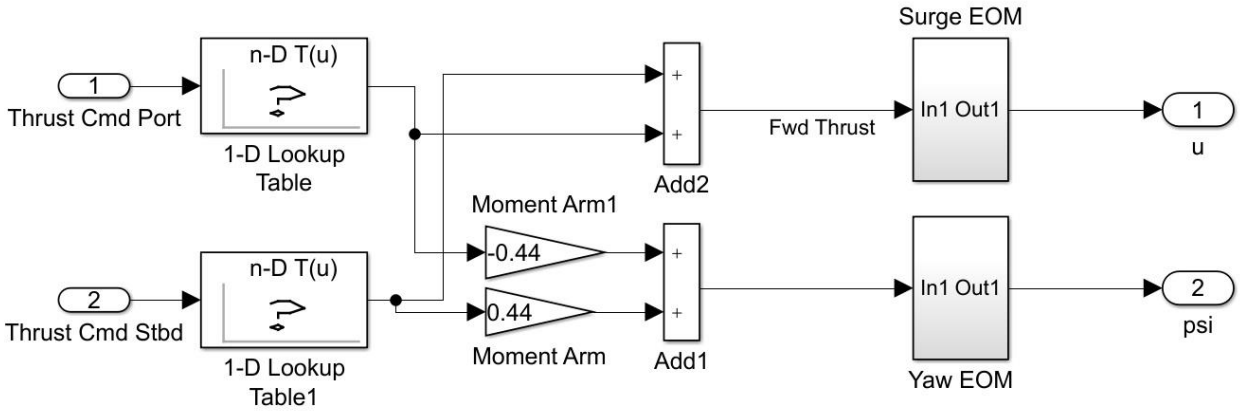

Figure 11. USV Simulation Model—Sub-Layer

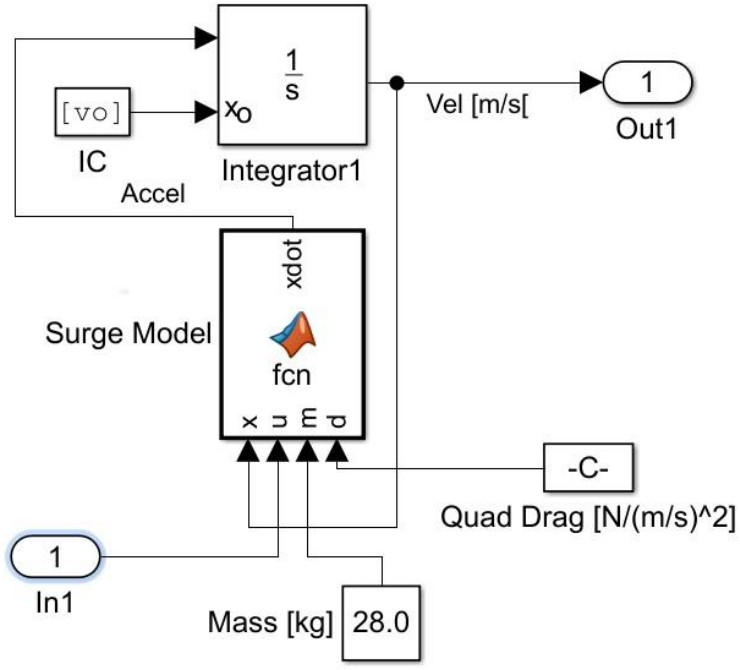

Figure 12. USV Equations of Motion—Sub-Layer

B. MODEL VERIFICATION

A Simulink verification of the open-loop system (see Figure 13) was conducted to ensure validity of the USV model prior to conducting feedback control testing. Simulations

were conducted over a range of motor commands, [0.0 to 1.0], which were converted to forces utilizing the same relationship displayed in Figure 8. Table 6 displays the numerical results of these tests. This data was then compared to the experimental results from Manzini who had correlated steady linear and angular velocity to thrust generation from the KF-USV in order to estimate the drag coefficient. Manzini conducted three variations of curve fitting, $y_1(x) = ax^2$, $y_2(x) = ax^2 + bx$ and $y_3(x) = ax^2 + bx + c$, where x and y are the forward or angular velocity and thruster force or torque generation from two thrusters respectively and *a*, *b*, and *c* are the coefficients. The quadratic only form, $y(x) = ax^2$, formed the best fit for both cases and the coefficient, *a*, was the basis of the quadratic drag terms identified in Table 2. Figure 14 confirms and validates that the numerical model matches the assumptions stated in previous sections.

Table 6. Model Verification Results

Thrust Cmd	0.1	0.2	0.3	0.4	0.5	0.6	0.7	0.8	0.9	1.0
Force [N] , *y*	0.6	2.2	8.2	14.8	21.0	28.8	39.4	41.2	41.4	40.6
Lin. Vel. [m/s], *x*	0.1884	0.3608	0.6966	0.9358	1.1187	1.3054	1.5268	1.5612	1.5647	1.5499
Torque[N*m], *y*	0.1320	0.4840	1.8040	3.2560	4.6200	6.3360	8.6680	9.0640	9.1080	8.9320
Ang. Vel. [rad/ s], *x*,	0.0308	0.059	0.1139	0.1529	0.1823	0.2134	0.2497	0.2553	0.2559	0.2535

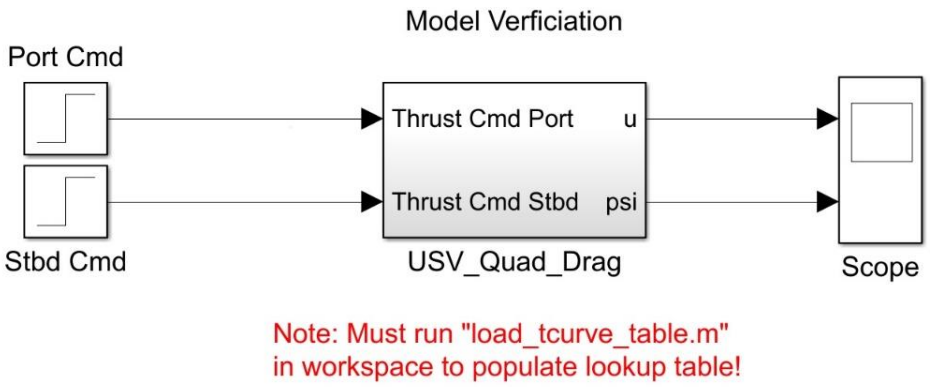

Figure 13. Open-Loop USV Model

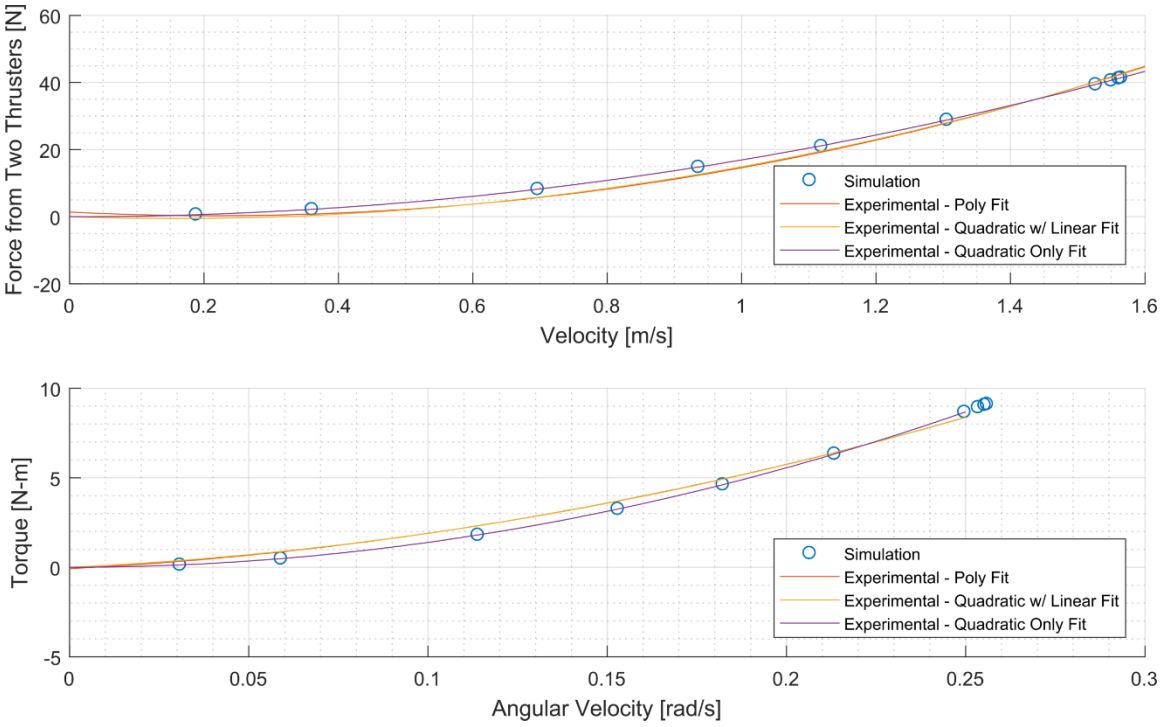

Figure 14. Model Verification Results

C. DECOUPLED DYNAMICS

The first set of testing conducted after the model verifications was on the decoupled system, designing and assessing heading (yaw) and speed (surge) control independently.

1. Heading Control

The basis for decoupled heading control was to analyze a 45-degree step input with zero forward velocity using simple feedback and a PID controller. We first tested and tuned the simple PID controller for the linear thrust relationship and then for the non-linear thrust relationship. Heading control was systematically tested and analyzed for trends utilizing the tuning approach presented in Table 5. Figures 15 and 16 display the effect of the heading controller operating on both the linear and non-linear thrust models, respectively. The plots are organized from top-to-bottom to show the effects of varying the proportional-only, integral-only, and derivative-only gains. The magnitude of proportional gain for the integral and derivative plots is 1.0.

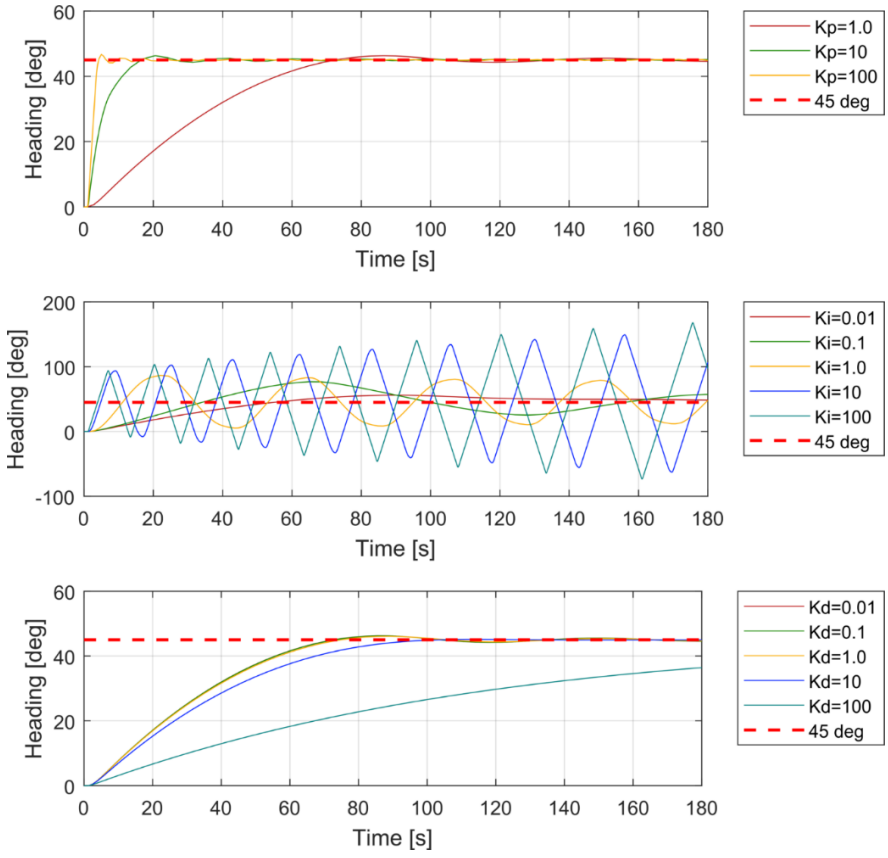

Figure 15. Tuning Step Responses—Heading Control—Linear Thrust Model Approximation

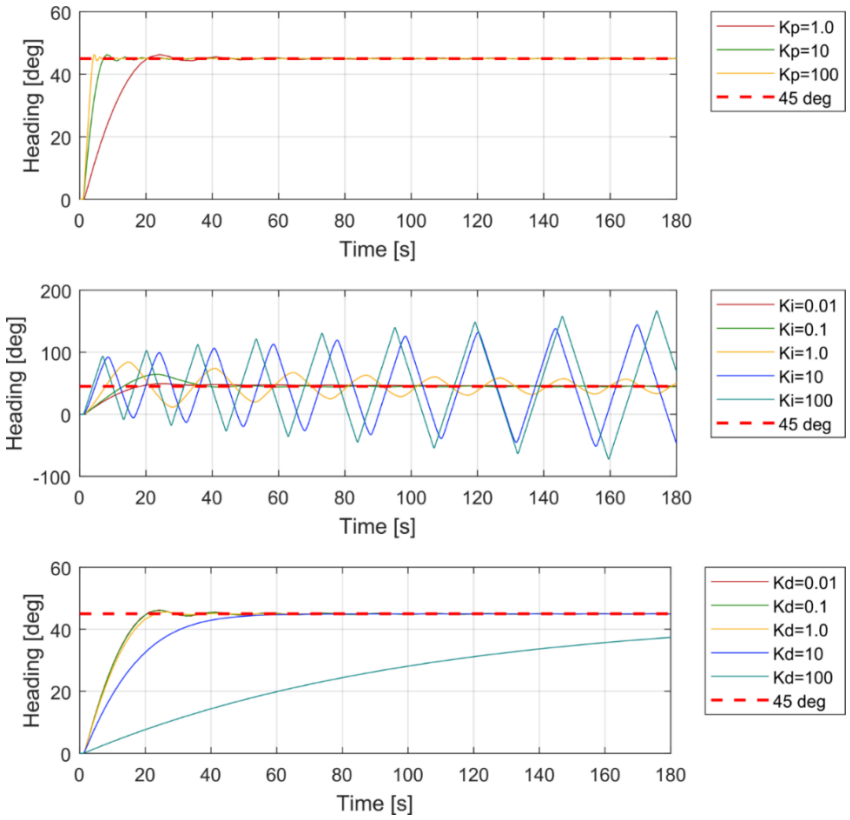

Figure 16. Tuning Step Responses—Heading Control—Non-Linear Thrust Model Approximation

From the figures, we can identify the following common trends:

1. Increasing the proportional gain improves response time but increases overshoot.

2. Increasing the integral gain drives the system unstable and should be set near zero. A non-expected result was the non-linearity of this response while unstable. Due to this system responding as predicted to a PD controller, the cause of abnormality was not investigated further.

3. Increasing the derivative gain slows system response and decreases overshoot.

4. The system responds best to a PID controller most closely resembling a Proportional-Derivative (PD) controller. This is expected due to the yaw

model having the form of a second order system, which includes a pure integrator.

Table 7 compares the performance characteristics of linear (L) and non-linear (NL) thrust model step responses from the proportional (top plot) and derivative (bottom plot) controllers shown in Figures 15 and 16. As this data indicates, even before fine-tuning the controllers, the non-linear thrust model presents advantages over the linear approximation in terms of rise time, T_R, settling time, T_S and percent overshoot, *OS*.

Table 7. Heading Control—Linear and Non Linear Thrust Model Approximation—Step Response Characteristic Comparison

Gains		***Rise Time,* T_R [s]**			***Settling Time,* T_S [s]**			***Overshoot, OS* [%]**		
Kp	**Kd**	**L**	**NL**	**Δ [s]**	**L**	**NL**	**Δ [s]**	**L**	**NL**	**Δ [%]**
1	0	51.0	13.40	**37.60**	70.00	26.80	**43.20**	2.00	3.20	**1.20**
10	0	9.9	4.30	**5.60**	31.90	9.00	**22.90**	2.40	3.00	**0.60**
100	0	2.2	2.20	**0.00**	7.70	4.60	**3.10**	3.90	2.90	**1.00**
1	0.01	51.0	13.40	**37.60**	70.10	26.70	**43.40**	2.00	3.10	**1.10**
1	0.1	51.1	13.50	**37.60**	70.30	26.60	**43.70**	1.90	3.00	**1.10**
1	10	61.6	28.70	**32.90**	88.20	48.40	**39.80**	0.00	0.00	**0.00**
1	100	76.9	76.90	**0.00**	97.00	96.70	**0.30**	0.00	0.00	**0.00**

When optimally tuned however, the controllers displayed near identical performance (see Figure 17) as numerical results show in Table 8. The responses are near overlapped with the non-linear curve exhibiting slightly less overshoot.

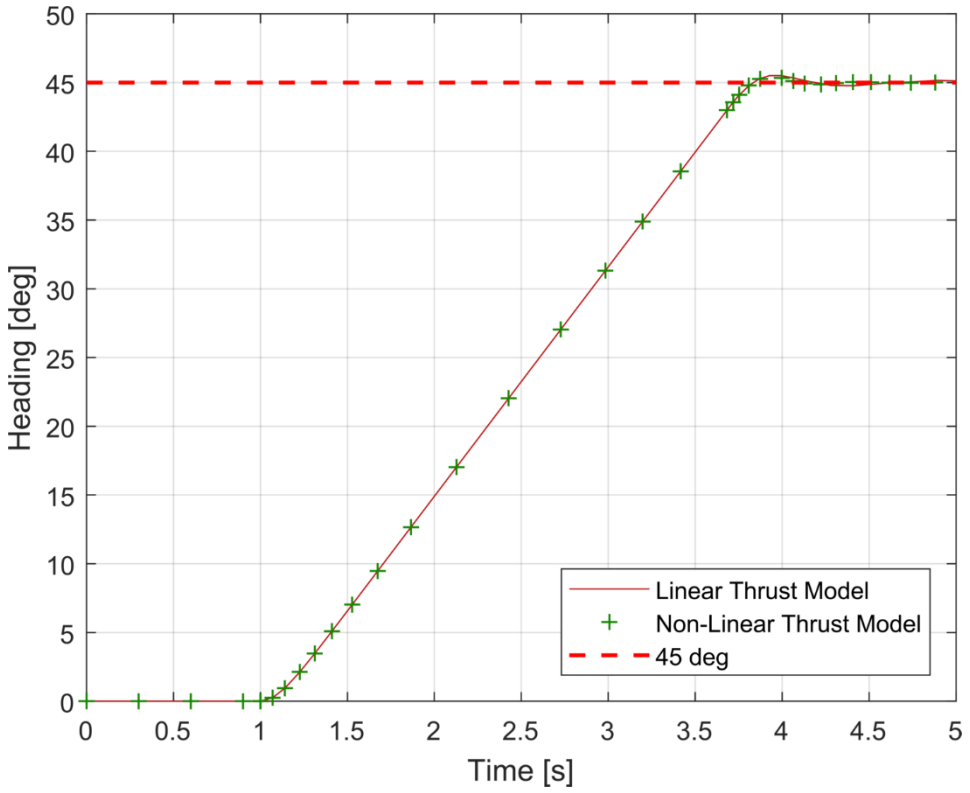

Figure 17. Heading Control—Optimized Step Response—Linear and Non-Linear Thrust Model Approximations

Table 8. Heading Control—Optimized Controller—Step Response Characteristic Comparison

Gains			***Rise Time,* T_R [s]**			***Settling Time,* T_S [s]**			***Overshoot, OS* [%]**		
Kp	**Ki**	**Kd**	**L**	**NL**	**Δ [s]**	**L**	**NL**	**Δ [s]**	**L**	**NL**	**Δ [%]**
1000	0.01	50	2.16	2.16	**0.00**	3.75	3.75	**0.00**	1.2	0.8	**0.4**

2. Speed Control

The basis for decoupled speed control was to analyze the closed-loop response to a low-speed (0.0 to 0.25 [m/s]) and high speed (1.25 to 1.50 [m/s]) step command independently. We tested each of these speed regions both with and without a feed-forward component, each while using either a linear or non-linear thrust model approximation. The goal of this simulation is to determine the effectiveness of like controller arrangements

over the full spectrum of speed commands (from low to high speed) and their effects on each speed region.

a. Low Speed Testing

(1) Linear versus Non-Linear Thrust Model Comparison

First, the low-speed region was tested according to the gain schedule of Table 5 in order to compare the linear and non-linear thrust model approximation and identify significant trends. Figures 18–19 display these results and are organized from top-to-bottom to show the effects of varying the proportional-only, integral-only, and derivative-only gains, respectively. From these figures, we observe the following trends common to both systems:

1. Increasing the proportional gain improves the system response.

2. A positive non-zero integration gain is necessary to reduce steady state error but can increase overshoot and oscillations.

3. A small derivative gain ($K_d << 1$) has negligible effect on system response but a gain larger than a factor of 10 increased system response but also increased steady state error.

4. The system responds best to a PID controller most closely resembling a Proportional-Integral (PI) controller.

Table 9 compares the performance characteristics of linear (L) and non-linear (NL) step responses from the proportional (top plot) and integral (middle plot) in Figures 18 and 19.

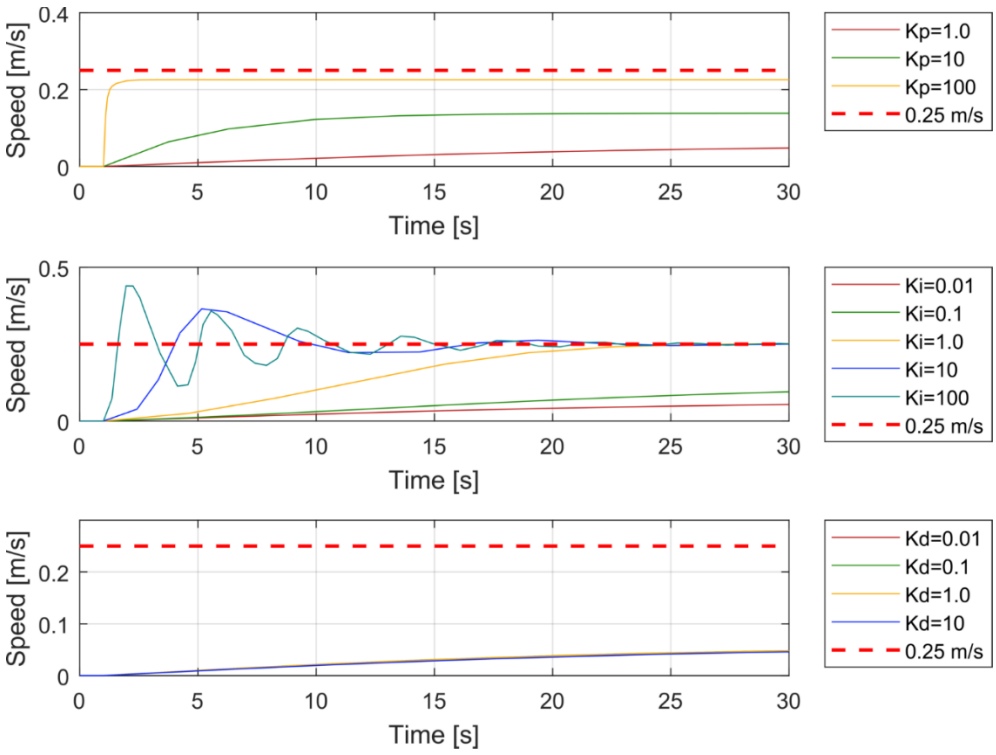

Figure 18. Tuning Step Responses—Low-Speed—Linear Thrust Model Approximation

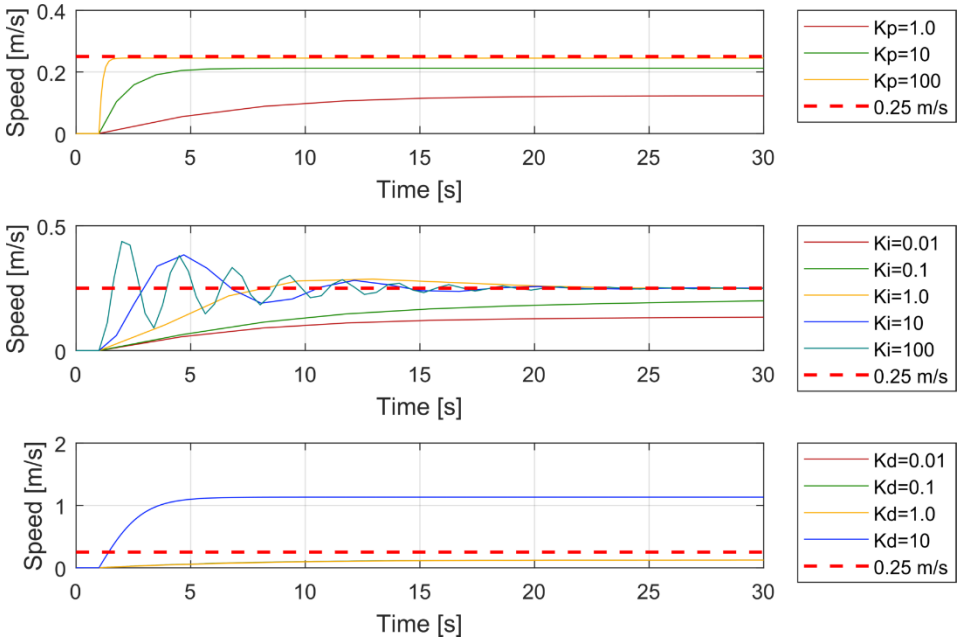

Figure 19. Tuning Step-Responses—Low Speed Control—Non-Linear Thrust Model Approximation

Table 9. Performance Characteristic Comparison—Low-Speed Control—Linear and Non Linear Thrust Model Approximation

Gains		***Rise Time,* T_R [s]**			***Settling Time,* T_S [s]**			***Steady State Error* [m/s]**		
Kp	**Ki**	**L**	**NL**	**Δ [s]**	**L**	**NL**	**Δ [s]**	**L**	**NL**	**Δ [m/s]**
1	0	33.2	11.49	**21.69**	56.73	20.71	**36.02**	0.19	0	**0.07**
10	0	9.1	2.36	**6.71**	16.67	5	**11.30**	0.11	0	**0.07**
100	0	0.3	0.30	**0.02**	1.87	2	**0.32**	0.02	0	**0.02**
1	0.01	58.5	45.26	**13.21**	91.62	88	**3.19**	0.17	0	**0.08**
1	0.1	66.7	43.36	**23.32**	93.92	82	**11.68**	0.09	0	**0.08**
1	1	14.9	5.09	**9.80**	23.96	22	**2.21**	0.00	0	**0.00**
1	10	1.7	1.47	**0.23**	21.52	21	**0.70**	0.00	0	**0.00**
1	100	0.4	0.41	**0.06**	23.93	22	**1.97**	0.00	0	**0.00**

Similar to the heading control, the non-linear thrust model approximation provides better system performance than the linear thrust model with respect to rise time, settling time, and steady state error, for the same test points. When the proportional and integral gains are increased by a factor of 100 independently, the system's rise times and steady-state errors converge but the non-linear thrust model demonstrates improved settling time performance. In addition, just as we observed with the heading controller, the speed controller's performance as their controllers are optimized through tuning. Figure 20 shows optimized responses and Table 10 shows the performance characteristics of each response.

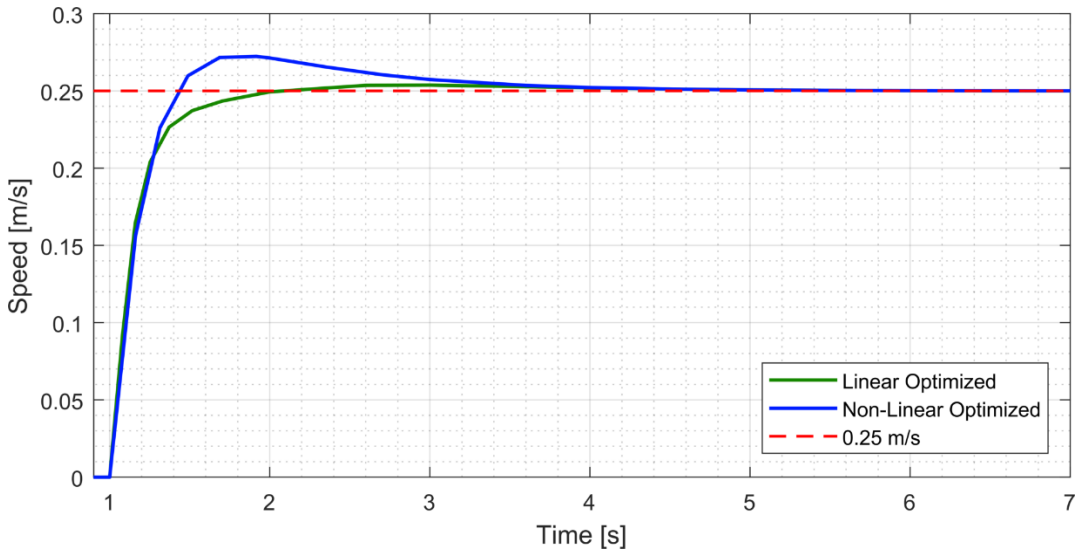

Figure 20. Optimized Step Responses—Low-Speed Control—Linear and Non-Linear Thrust Model Approximations

Table 10. Optimized Performance Characteristics Comparison—Low-Speed Control—Linear and Non-Linear Thrust Model Approximations

Gains			***Rise Time, T_R* [s]**			***Settling Time, T_S* [s]**			***Overshoot [%]***		
Kp	**Ki** (L/NL)	**Kd**	**L**	**NL**	**Δ[s]**	**L**	**NL**	**Δ[s]**	**L**	**NL**	**Δ[%]**
100	80/100	0.01	0.65	0.25	**0.40**	1.97	3.06	**1.09**	0.29	7.32	**7.23**

(2) Feed-Forward Compensation Testing

Next, we simulated this system both with and without a feed-forward term. As previously discussed, and graphically displayed in Figure 6, our definition of feed-forward compensation is an example of command-compensated control. Therefore, based on an empirically measured relationship of thrust force to velocity for a range of set-points, we can predict certain dynamics of the response and use them advantageously. In this research, we assume that we understand the relationship between commanded velocity and the thrust required to achieve it, based on (4). If we assume steady-state velocity (i.e. $\dot{u} = \frac{du}{dt} = 0$), then the thrust required, X_C , is a relationship between the drag components and commanded velocity expressed as

$$X_C = \cancel{M_{RB}\dot{u}} + (X_{|u|u}|u| + X_u)u \tag{9}$$

Then, by incorporating the appropriate drag coefficients from Table 2, our relationship is reduced to

$$X_C = \left[16.9|u| + \cancel{X_u}\right]u = 16.9|u|u \tag{10}$$

for the total thrust needed for two thrusters. Figure 21 provides one example of a Simulink model designed for this simulation that incorporates this feed forward relationship.

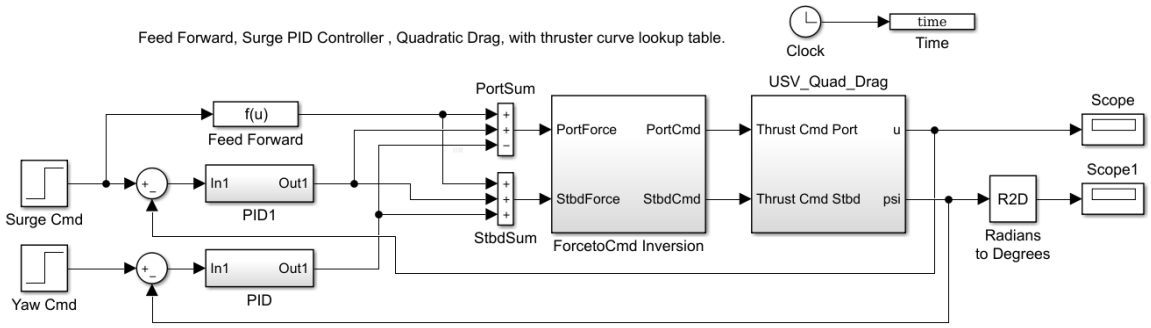

Figure 21. Speed Control with Feed-Forward Architecture in Simulink Model

For this evolution, we utilized a non-linear thrust model approximation and conducted the same systematic tuning steps (see Table 5 for gain schedule) to serve as a basis for comparison. In addition to observing the step-response and accompanying characteristics, the integrator's effort was also recorded to analyze the effect of integrator wind-up. Figures 22–23 display these results and are organized from top-to-bottom to show the effects of varying the proportional-only, integral-only, and derivative-only gains respectively. From these figures, we observe that both systems demonstrate the same trends as the speed-controller discussed in the previous section, performing best with a PI controller. This is expected as the model of the plant is identical and the feed forward component does not change the inherent dynamics of the plant. Table 11 compares the performance characteristics of the non-feed-forward (NF) and the feed-forward (FF) step responses from the proportional and integral plots in Figures 22–23.

Table 11. Performance Characteristics Comparison—Low-Speed Control—Feed Forward Compensation

Gains		***Rise Time, T_R* [s]**			***Settling Time, T_S* [s]**			***Steady State Error* [m/s]**		
Kp	**Ki**	**NF**	**FF**	**Δ [s]**	**NF**	**FF**	**Δ [s]**	**NF**	**FF**	**Δ [m/s]**
1	0	11.49	8.97	**2.52**	20.71	16.17	**4.54**	0.13	0.00	**0.13**
10	0	2.36	2.95	**0.59**	5.37	6.18	**0.81**	0.04	0.00	**0.04**
100	0	0.30	0.40	**0.10**	1.55	1.70	**0.14**	0.01	0.00	**0.01**
1	0.01	45.26	8.98	**36.28**	88.43	16.16	**72.26**	0.09	0.00	**0.10**
1	0.1	43.36	8.53	**34.84**	82.24	14.27	**67.97**	0.01	0.00	**0.01**
1	1	5.09	3.85	**1.24**	21.75	23.98	**2.23**	0.00	0.00	**0.00**
1	10	1.47	1.43	**0.04**	20.82	28.17	**7.35**	0.00	0.00	**0.00**
1	100	0.41	0.51	**0.10**	21.96	29.30	**7.34**	0.00	0.00	**0.00**

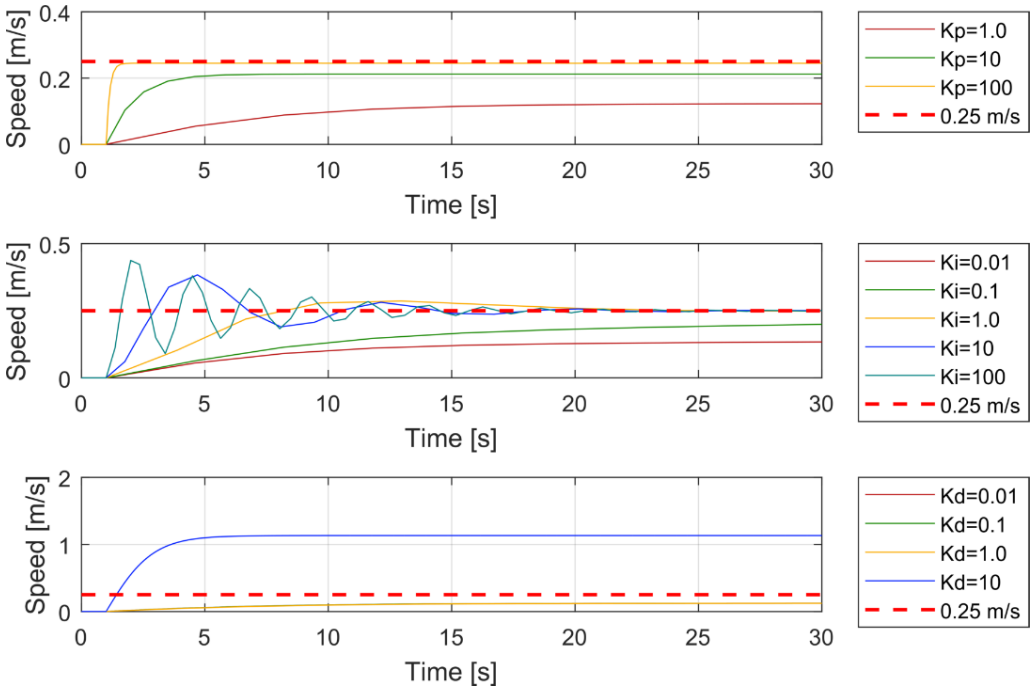

Figure 22. Tuning Step Responses—Low-Speed Control without Feed-Forward Compensation

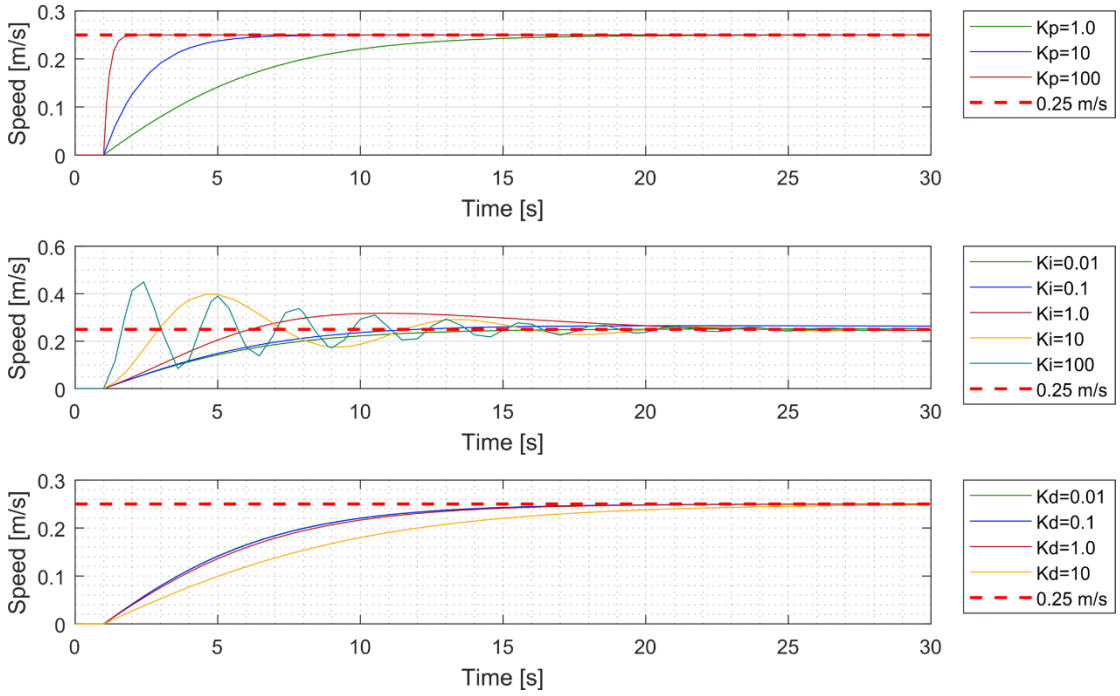

Figure 23. Tuning Step Responses—Low-Speed Control with Feed-Forward Compensation

The feed-forward compensation does provide benefit without increased tuning in system response. This is measured in decreases in rise times and steady state error for identical tuning. As the systems are tuned with greater effect, the benefits of feed-forward compensation disappear, as both systems achieve nearly identical performance characteristics. This is represented graphically in Figure 24 and numerically in Table 12.

Table 12. Optimized Performance Characteristics—Low-Speed Control—Feed-Forward Compensation

Gains			***Rise Time, T_R* [s]**			***Settling Time, T_S* [s]**			***Steady State Error [m/s]***		
Kp	**Ki** (NF/FF)	**Kd**	**NF**	**FF**	**Δ[s]**	**NF**	**FF**	**Δ[s]**	**NF**	**FF**	**Δ[m/s]**
100	10/0.01	0.01	0.31	0.30	**0.01**	1.61	1.54	**0.07**	0.00	0.00	**0.00**

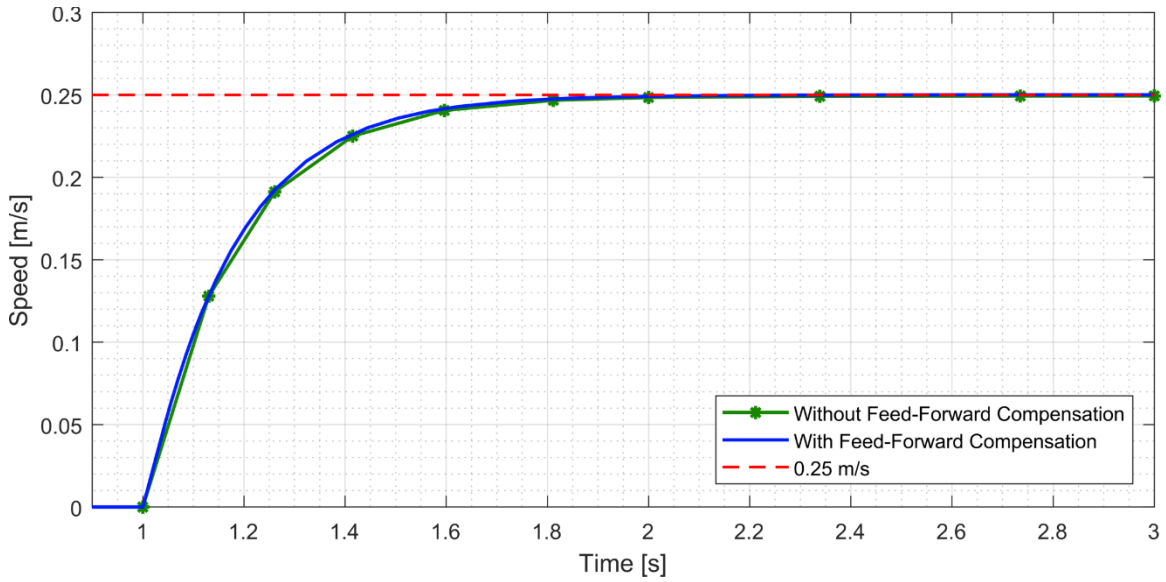

Figure 24. Optimized Step Response—Low-Speed Control—Feed Forward Control

The feed-forward compensation does provide decreased integrator effort and prevents integrator wind-up, as displayed in Figure 25. Specifically, the system without feed-forward compensation accumulated a large integral contribution before arriving at a steady state. This is indicative of wind up or over-accumulation of error that the system then has to resolve. The lack of integrator effect in the feed-forward response is expected in an ideal simulation setting, but this remains to be verified in an experimental setting where the feed-forward compensation may not be exact.

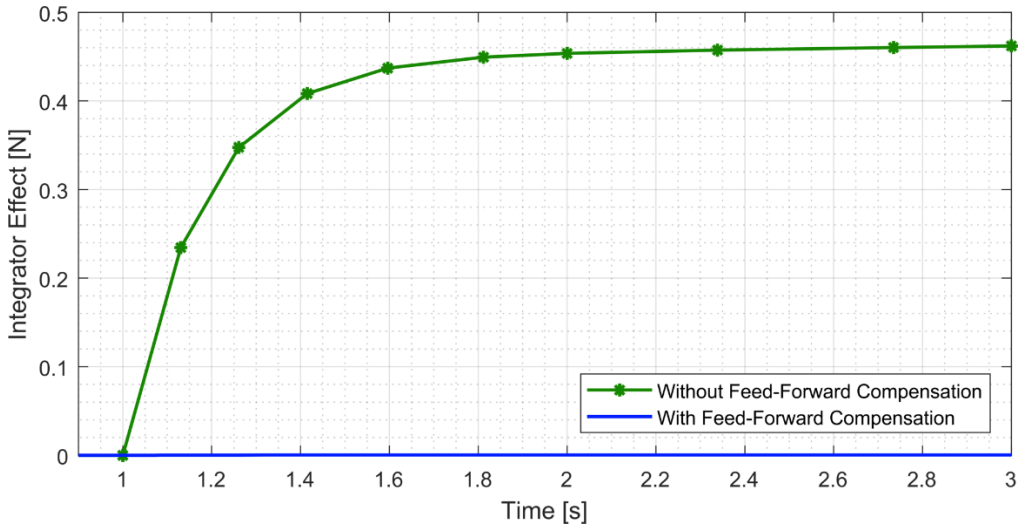

Figure 25. Optimized System Response—Feed-Forward Compensation—Integrator Effort Comparison

b. High-Speed Controller Testing

(1) Linear versus Non-Linear Thrust Model Comparison

First, the high-speed region, 1.25—1.50 [m/s], was tested according to the gain schedule of Table 5 to compare the linear and non-linear thrust model approximation for and identify significant trends. The step change was initiated after 60 seconds to allow for the system to first stabilize at the lower set point. Figures 26–27 display these results and are organized from top-to-bottom to show the effects of varying the proportional-only, integral-only, and derivative-only gains respectively. From these figures, it is clear that most of the controllers are inadequate and fail to reach a steady-state at the lower set-point. Comparing the step-responses for linear and non-linear thrust models does not reveal any appreciable performance differences. Since previous simulation results for this system suggest that it performs best with a PI controller, we simulated another series of tuning gains listed in identified in Table 13.

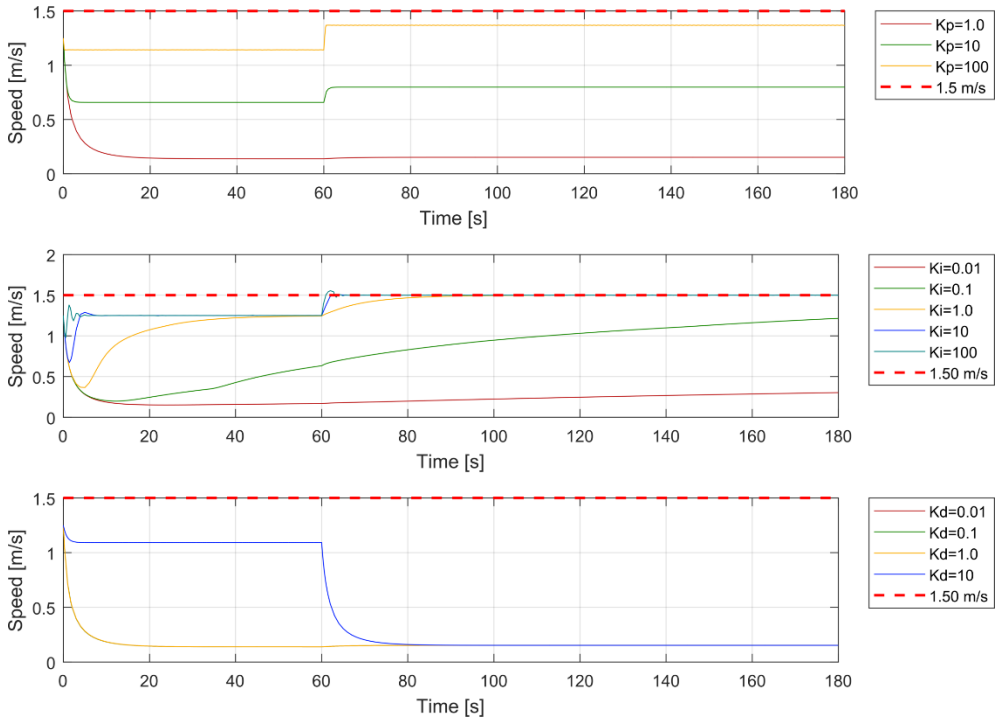

Figure 26. Tuning Step Responses—High-Speed—Linear Thrust Model Approximation

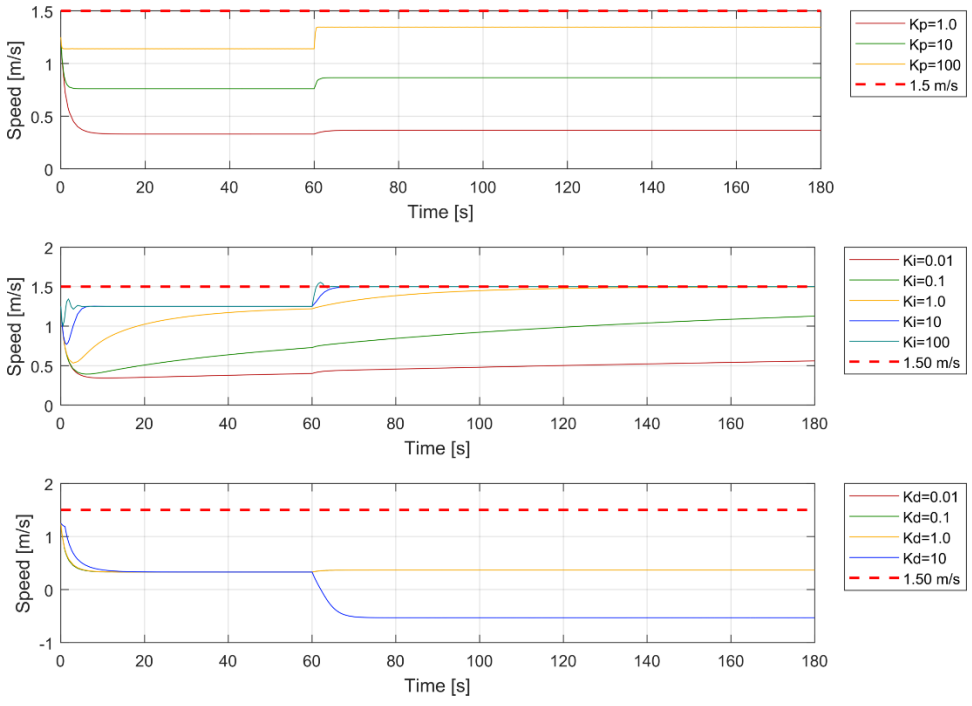

Figure 27. Tuning Step-Responses—High Speed Control—Non-Linear Thrust Model Approximation

Table 13. High Speed Control—Refined Tuning Gain Table

Test #	K_P	K_i	K_d
14	100	100	0
15	100	250	0
16	100	500	0
17	100	750	0
18	100	1000	0

Using this tuning schedule, the systems were re-tested and their results are plotted in Figure 28 where the linear thrust approximation is located in the top plot and the non-linear thrust approximation in the lower plot. These suggests that while the non-linear thrust model approximation offers some advantages in systems response, the discernable performance differences between thrust models in the high-speed region are much smaller than they were in the low-speed region.

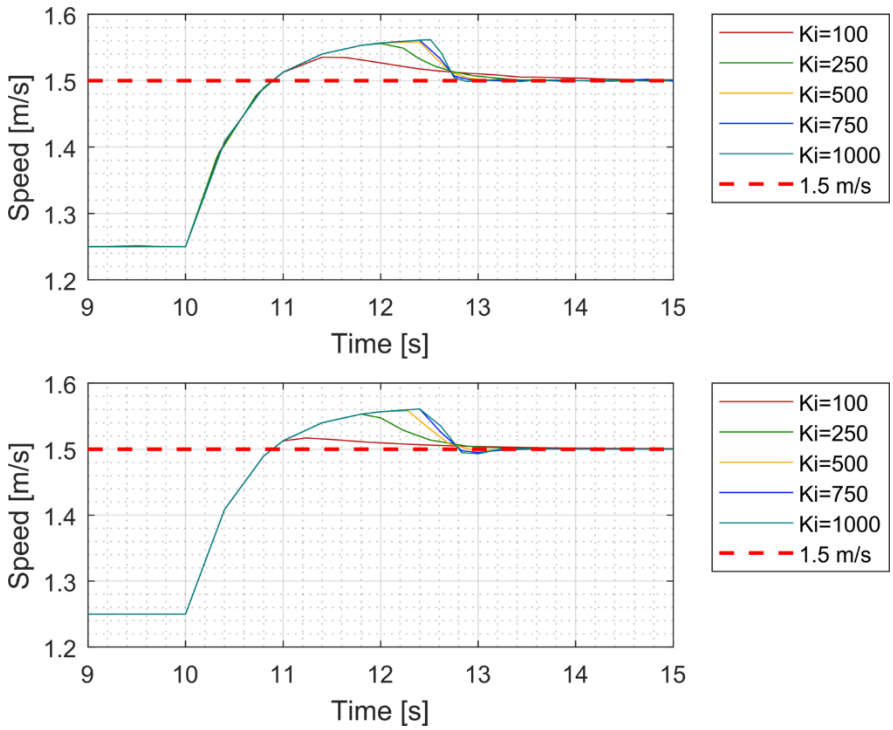

Figure 28. Tuning Step-Response—High-Speed Control—Second Gain Testing Iteration

Figure 29 and Table 14 provide the graphical and numerical representations of the optimally-tuned step responses for both systems. As expected, their responses are nearly identical. However, this information will be helpful for understanding the relative advantages of using different controllers across a larger velocity spectrum.

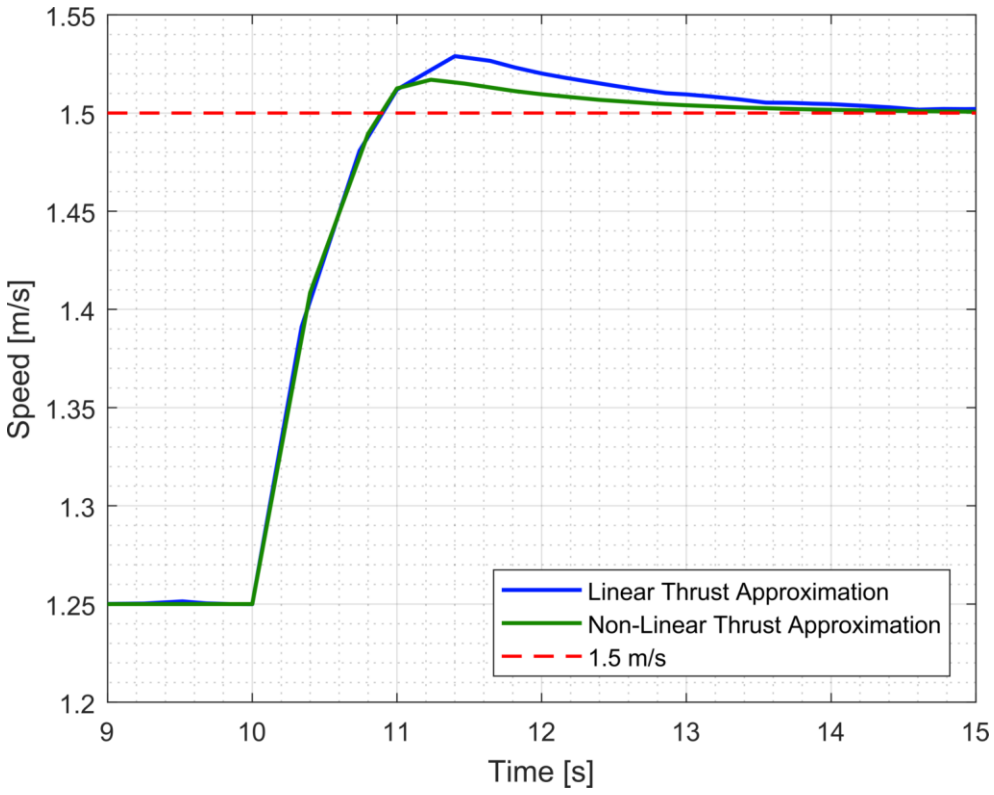

Figure 29. Optimized Step-Response—High-Speed—Linear and Non-Linear Thrust Model Approximations

Table 14. Optimized Performance Characteristics—High Speed—Linear and Non-Linear Thrust Model Approximations

Gains			***Rise Time, T_R* [s]**			***Settling Time, T_S* [s]**			***Overshoot [%]***		
Kp	**Ki** (L/NL)	**Kd**	**L**	**NL**	**Δ[s]**	**L**	**NL**	**Δ[s]**	**L**	**NL**	**Δ[%]**
100	80/100	0.01	0.65	0.65	0.00	1.97	1.96	0.01	0.28	0.10	0.18

(2) Feed-Forward Compensation Testing

For the high-speed region, we assume the same architecture and relationships for a feed forward compensator as in the low-speed region. We also conducted the same systematic tuning steps as discussed in previous sections (see Table 5 for gain schedule) to serve as a basis for comparison. In addition to observing the step-response and its accompanying characteristics, the integrator's effort was also recorded to analyze the effect of integrator wind-up. Figures 30–31 display these results and are organized from top-to-bottom to show the effects of varying the proportional-only, integral-only, and derivative-only gains respectively. From these figures, we can observe that the feed-forward compensation provides significant benefit to the system. Comparing the plots of the proportional gain iterations of both systems shows that the base feedback system response (i.e., $K_P = 1$) of the system with feed-forward compensation quickly reaches steady states near both set points, 1.25 and 1.50 [m/s], without steady state error. Whereas, the system without feed-forward compensation is under-actuated and unable to respond to changes in speed commands. This advantage is consistent across the various tuning gains and controller effects.

For the optimized system responses, displayed in Figure 32, the feed-forward compensated system has a near identical response, but it exhibits less overshoot and a faster settling time (see Table 15).

Additionally, the compensated system provides decreased integrator effort and prevents integrator wind-up shown in Figure 33. The integrator for the uncompensated system is consistently accumulating error in order to maintain a high speed steady state, whereas the compensated system's integrator effort is minimized to zero.

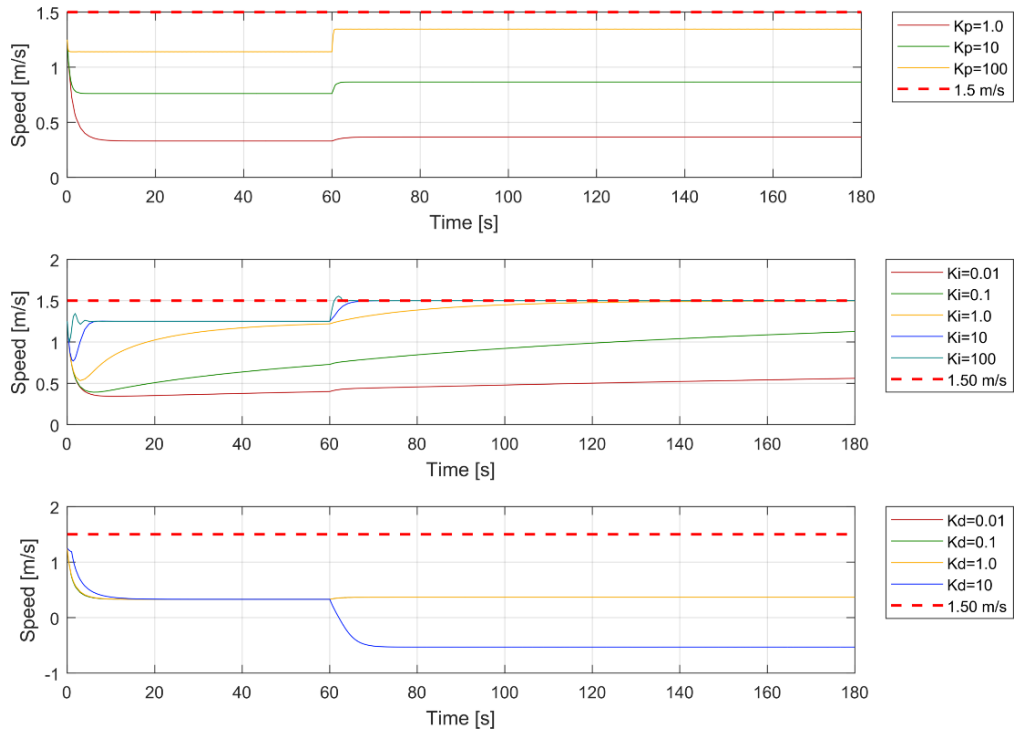

Figure 30. Tuning Step Responses—High-Speed Control without Feed-Forward Compensation

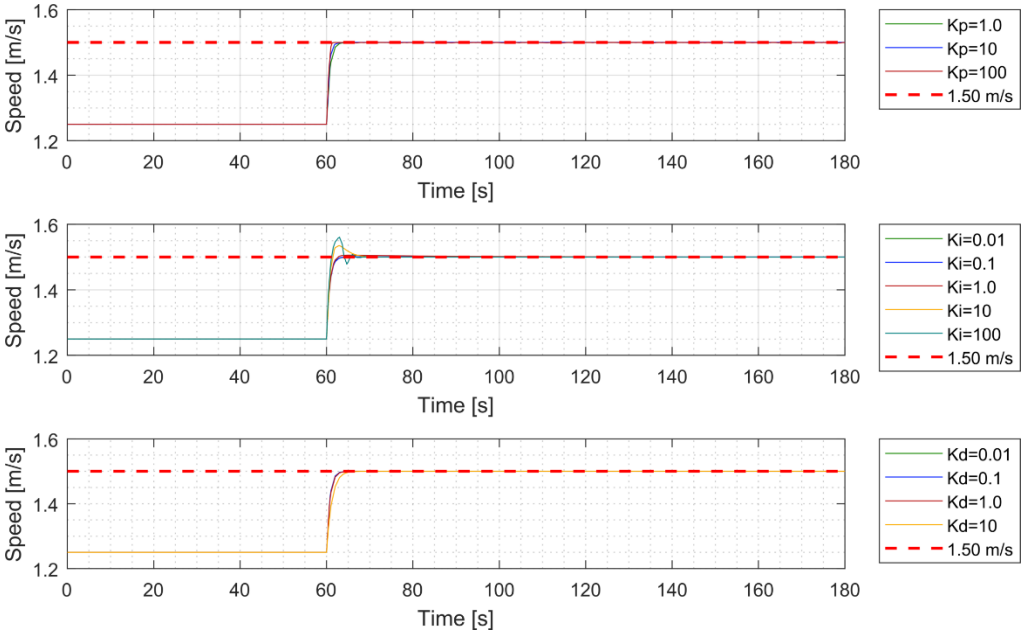

Figure 31. Tuning Step Responses—High-Speed Control with Feed-Forward Compensation

Table 15. Optimized Performance Characteristics—Low-Speed Control—Feed-Forward Compensation

Gains			***Rise Time, T_R* [s]**			***Settling Time, T_S* [s]**			***Overshoot [%]***		
Kp	**Ki** (NF/FF)	**Kd**	**NF**	**FF**	**Δ[s]**	**NF**	**FF**	**Δ[s]**	**NF**	**FF**	**Δ[%]**
100	100/1	0.01	0.65	0.68	**0.03**	1.96	1.93	**0.03**	2.11	0.24	**1.87**

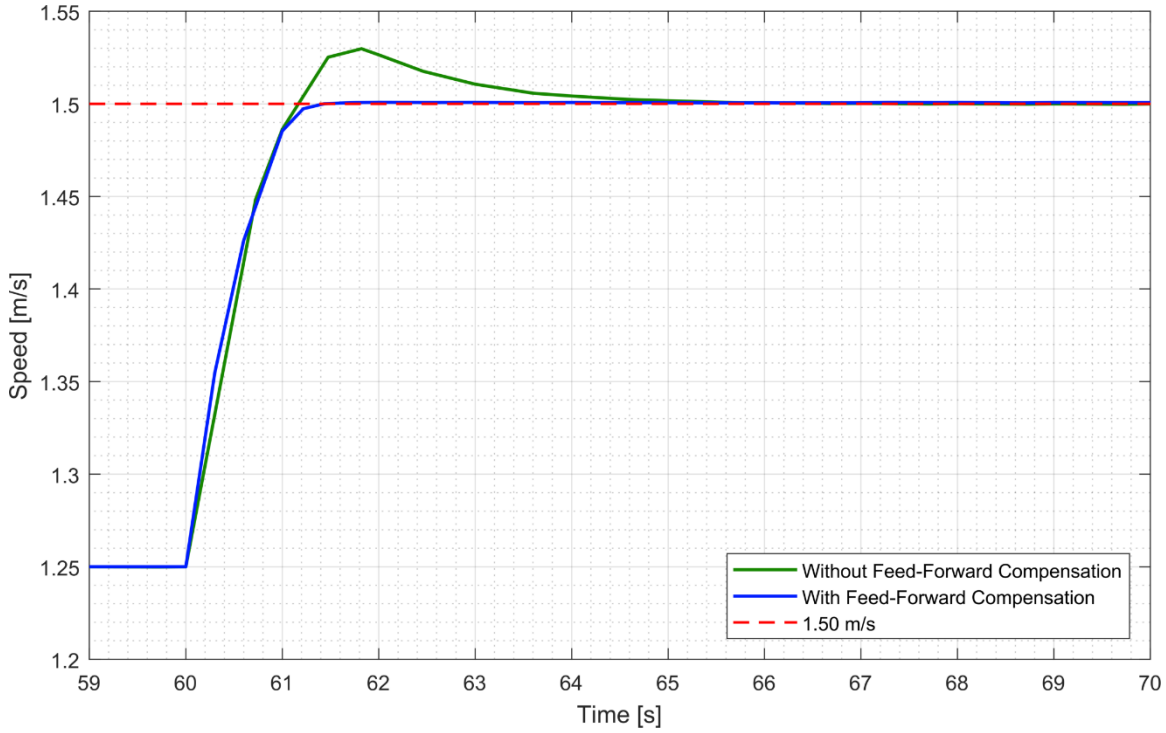

Figure 32. Optimized Step Response—High-Speed Control—Feed Forward Control

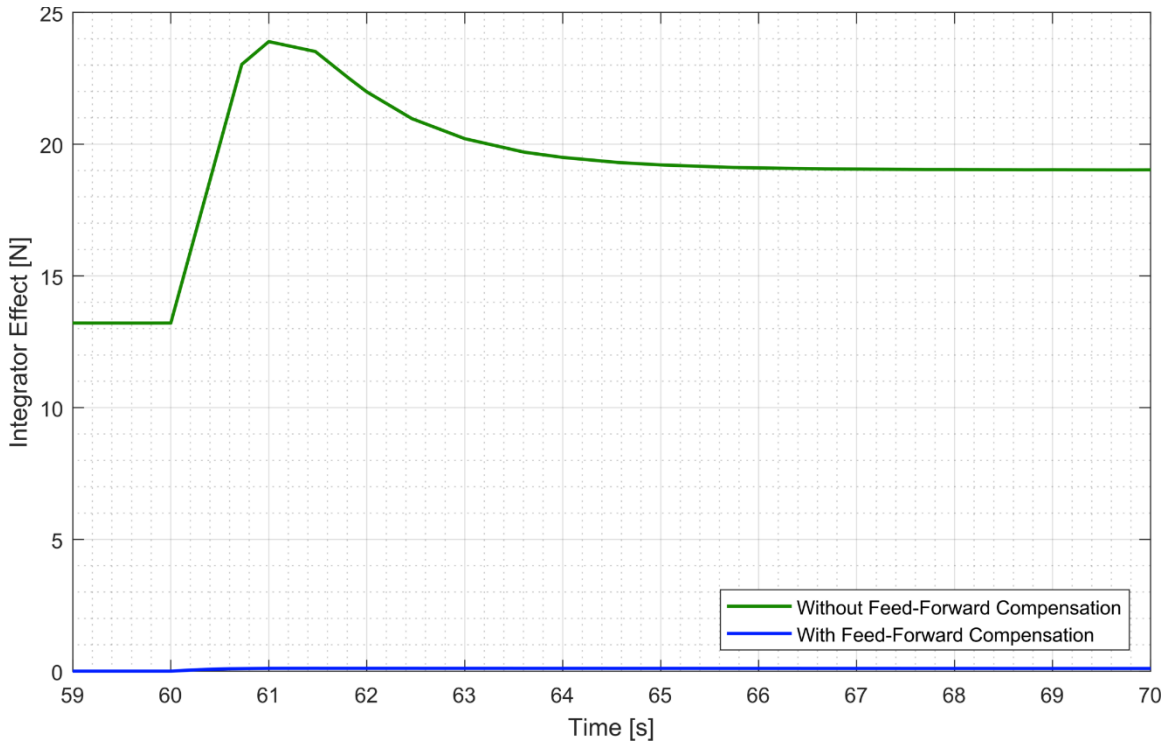

Figure 33. Optimized System Response—Feed-Forward Compensation—Integrator Effort Comparison

D. COUPLED DYNAMICS

For the plant model with coupled dynamics, we simulated the KF-USV conducting a 45 degree turn at a steady-state low speed, 0.25 [m/s], and at a steady-state high speed, 1.25 [m/s]. Results from multiple simulations were used to analyze the effects of linear and non-linear thrust model approximations, feed forward compensation, and their combined configurations on heading and speed control during the vessel's maneuver.

a. Low Speed Turn

The low speed turn was simulated to compare the impacts of using different thrust models, as well as feed-forward compensation. For the heading controller, we selected the optimal gains identified during prior testing ($K_P = 1000$, $K_i = 0.01$, and $K_d = 50$). In the same way, the speed controllers were tuned using the optimized gains from the previous sections for each given configuration. For example, the linear thrust model approximation with no feed forward compensation utilized $K_P = 100$, $K_i = 80$, and $K_d = 0.01$. The

systems were then tested for each configuration with a step command of 45 degrees initiated at 10 seconds. Figure 34 displays the step response for the heading change and subsequent speed response of the vessel, as shown in the top and bottom plots, respectively. Key performance characteristics for heading step responses are identified in Table 16. Analyzing the low speed turn responses for each test case, we observe the following:

1. All configurations produce very similar responses to the step change in heading.

2. Heading changes caused a positive, then a negative speed surge for all of the test cases, before returning to the steady-state value of 0.25 [m/s].

3. All responses eventually achieved steady state values for the desired heading and speed commands.

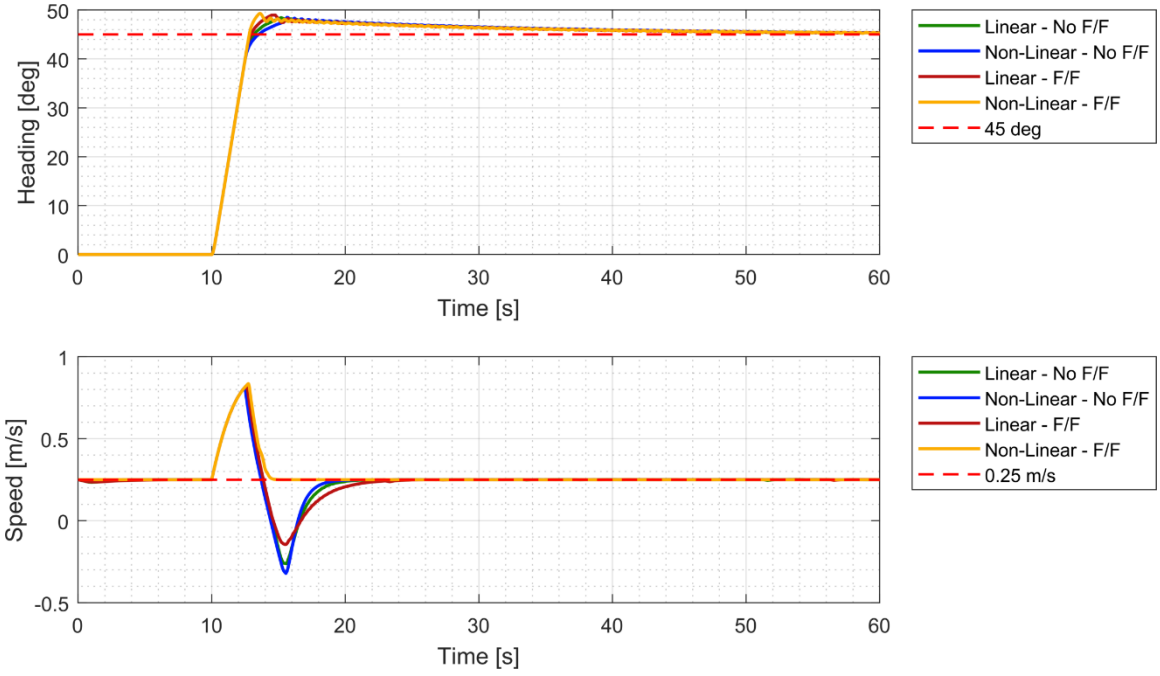

Figure 34. Coupled Dynamics System Responses—Low Speed Turn

Table 16. Coupled Dynamics—Low Speed Turn—Performance Characteristics Comparison—Heading Response

Surge Controller Gains			***Rise Time, T_R* [s]**	***Settling Time, T_S* [s]**	***Overshoot [%]***
Case	**Kp**	**Ki**	**L**	**L**	**L**
Linear / No Feed Forward	100	80	2.18	33.57	6.75
Non-Linear / No Feed Forward	100	20	2.17	33.53	8.90
Linear / Feed Forward	100	50	2.18	32.69	7.95
Non Linear / Feed Forward	100	0.01	2.18	32.72	8.59

The integrator effect on speed control was recorded and plotted in Figure 35. The systems which use feed forward compensation produce diminished or no integrator effect in order to maintain speed. The small amount of integrator associated effect produced when using the linear thrust model comes from tuning this system to use a larger integrator gain value.

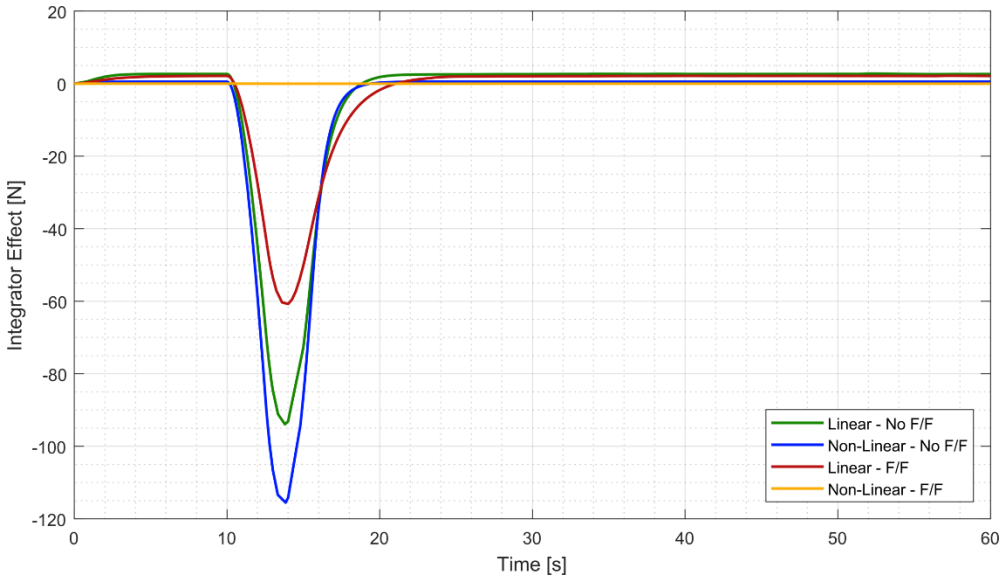

Figure 35. Low Speed Turn—Integrator Effort Comparison

b. High Speed Turn

The high speed turn control region was tested simulated to compare the impacts of using different thrust models, as well as feed-forward compensation. The systems were tuned using the same process used to tune the low speed turn, but for gain values associated with prior high speed testing. Figure 36 displays step response for the heading change and subsequent speed response of the vessel, as shown in the top and bottom plots, respectively. Key performance characteristics for heading step responses are identified in Table 17. Analyzing the high speed turn responses for each test case, we observe the following:

1. All configurations produce very similar responses to the step change in heading.

2. Feed forward compensation and a non-linear thrust model approximation had a significant effect on the system's speed response to the heading change. The other test configurations exhibited a negative, then a positive speed surge, before returning to steady state.

3. However, the non-linear thrust model with feed forward compensation returned to its steady state speed value without this positive speed overshoot.

4. All responses eventually returned to steady state values for heading and speed respectively.

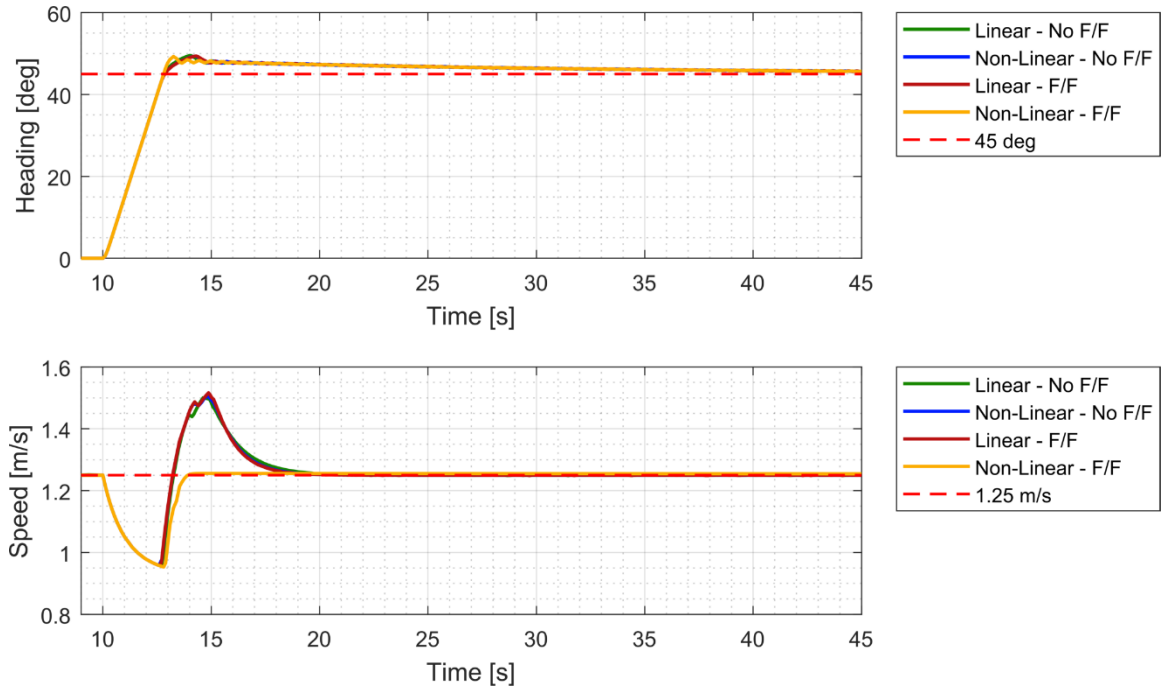

Figure 36. Dynamics System Responses—High Speed Turn

Table 17. High Speed Turn—Performance Characteristics Comparison—Heading Response

Surge Controller Gains			***Rise Time, T_R* [s]**	***Settling Time, T_S* [s]**	***Overshoot [%]***
Case	**Kp**	**Ki**	**L**	**L**	**L**
Linear / No Feed Forward	100	80	2.18	33.12	9.21
Non-Linear / No Feed Forward	100	100	2.18	32.68	8.84
Linear / Feed Forward	100	100	2.17	34.69	9.15
Non Linear / Feed Forward	100	1	2.17	33.53	8.78

Additionally, the integrator effect on speed control was recorded and plotted in Figure 37. The systems which use feed forward compensation produce diminished or no integrator effect to maintain speed. The small amount of integrator effect produced when using the linear thrust model comes from tuning this system to use a larger integrator gain value.

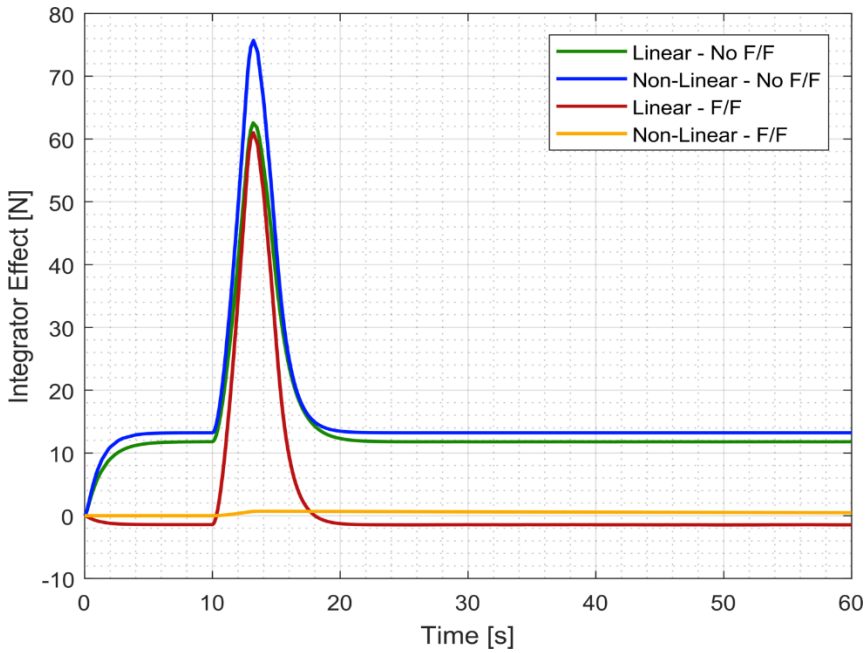

Figure 37. High Speed Turn—Integrator Effort Comparison

E. SIMULATION SUMMARY

From our simulation testing, we can draw general conclusions based on our choice of system/model, various controller architectures and ultimately the effects of individual techniques. We can also compare simulated responses to performance predictions that have been established.

1. As predicted, the heading controller demonstrated improved response when the PID controller was tuned to closely resemble a PD controller.

2. Speed control demonstrated improved response when the PID controller was tuned to closely resemble a PI controller.

3. The non-linear thrust model approximation did provide increases in performance consistency across the low and high speed regions when the systems were roughly tuned (at the same gains) to the linear thrust model approximation.

4. This benefit diminished when the systems were optimally tuned and then tested across both speed regions. This produced nearly identical performance.

5. As predicted the feed forward compensation produced better baseline performance in surge response for both low and high speed regions. In particular, the high speed simulation results revealed the feed forward as a significant performance enhancer for its ability to resolve steady state error.

Overall, the simulation provided feedback which was useful in framing expectations for the future experimental results and providing a basis for comparison. The controller techniques fundamentally performed as expected, but multiple simulations provided valuable information about the system itself.

THIS PAGE INTENTIONALLY LEFT BLANK

IV. EXPERIMENTAL RESULTS AND ANALYSIS

A. EXPERIMENTAL SETUP

1. Software and Controller Implementation

The KF-USV has onboard computer running Ubuntu Linux with a Robotic Operating System (ROS) middleware installed to support remote communication and diagnostic support. ROS is a common open-source software package in robotics and allows the KF-USV to be integrated with ROS-based sensors and remote networks. A ROS system architecture is based on defining a 'ROS Master' which allows individual pieces of software or 'nodes' to find and communicate with each other through the publishing or subscribing of 'topics' via standardized message templates. This architecture allows for the remote implementation of a low-level controller for the KF-USV as an alternative to implementing the algorithm directly on the vessel. Therefore, this research utilized MATLAB and Simulink for controller design and implementation.

Using the same Simulink models for heading and speed controllers that we developed previously made it possible to replicate our simulation process on the actual KF-USV system. Whereas the inputs and outputs affecting feedback in simulation were computed from a mathematical model of the vehicle's equations of motion, the experimental controllers subscribed to topics containing KF-USV sensor data and published topics containing KF-USV thruster commands via a local wireless network. Figure 38 displays one iteration of a Simulink model used in this research utilizing this ROS based publish and subscribe architecture. Using Simulink to communicate with ROS over a wireless network requires careful selection of the frequencies at which the Simulink controller publishes messages to the ROS Master. Simulink is able to process its operations at a significantly faster rate than the KF-USV can receive and execute commands. Therefore, Simulink's default solver settings are adjusted from variable-step to fixed-step with step-size limited to 0.1 seconds, correlating to a refresh rate of 10 Hz. Additionally, we used the Real-Time Pacer [24] block, a third-party Simulink tool to synchronize Simulink execution with the host computer's real-time clock.

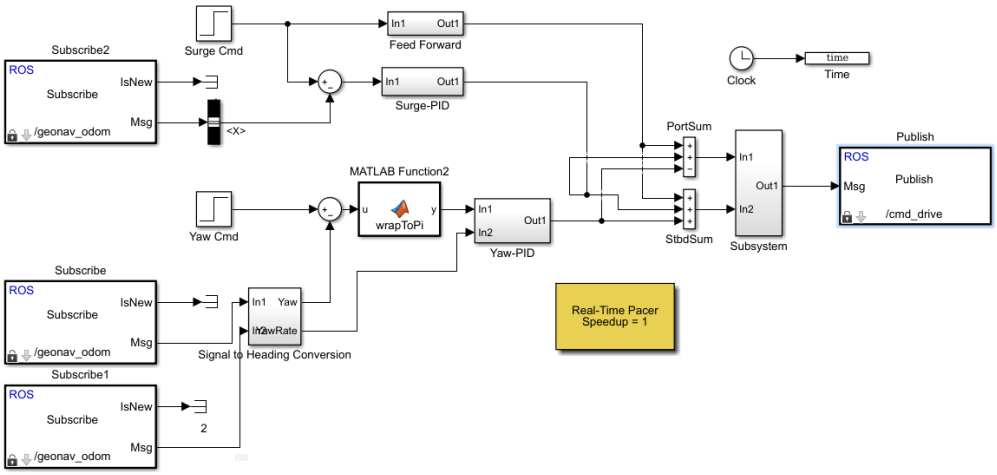

Figure 38. Simulink Model of Controller with ROS Functionality

2. Sensor Integration and Feedback Management

As previously mentioned, an advantage of utilizing a ROS middleware is the integration of any supported by existing ROS packages (i.e., drivers) with well-defined software modules (nodes), publish/subscribe topics, and message definitions. This allows the KF-USV to be modular and dynamic in terms of what sensors can be integrated to support controller, path-planning, and guidance development. For this research, sensor-integration requirements were minimum and included only one addition from the base model. This was a LORD MicroStrain 3DM®-GX5-45 GNSS-aided inertial navigation system (INS) for positional and dynamic measurements. Equipped with its own Kalman filtering algorithms, this sensor was chosen for its improved inertial measurement accuracy and advantages for sensitive control. The aforementioned Simulink controllers subscribed to the velocity, yaw and yaw rate messages published by the MicroStrain ROS package [25] for feedback control. This information also served as the basis for experimental analysis and was recorded to the MATLAB workspace. Table 18 lists the ROS nodes, topics and messages that were utilized for this research.

Table 18. ROS Nodes, Topics and Messages of Interest for Research

Equipment (Node)	/Topic /Message	Purpose
MicroStrain INS	/geonav_odom /nav_msgs/Odometry	Subscribed. Utilized for linear 'X' velocity (surge), heading (yaw) angle and turn rate (yaw rate).
KF-USV Motor Control Unit (MCU)	/cmd_drive /kingfisher_msgs/ Drive	Published. Utilized to send motor control commands [-1 to 1] for port and starboard units.

3. Test Site Locations

The experimental testing of controller design techniques with the KF-USV took place in two locations in Monterey, California: (1) at the Naval Postgraduate School's Center for Autonomous Vehicle Research (CAVR) test tank, and (2) Lake El Estero.

a. CAVR Test Tank

The CAVR test tank, pictured in Figure 39, was utilized to conduct testing associated with decoupled heading control. It provides a small experimental testing location with negligible environmental effects such as wind and currents. It is 6.10 meter long, 4.57 meter wide, and 2.13 meter deep and filled with freshwater. For safety of the vessel, the KF-USV was attached to an electro-mechanical chain fall with slack placed in the chain to allow for freedom of movement but to prevent the vessel from colliding with the walls. The chain-fall created some inconsistencies during experimental runs as the vessel, due to its dynamics, inherently surges when turning. The chain fall retarded this motion, causing oscillations during heading step response testing. Nevertheless, this location was still valuable for developmental testing. It improved understanding of the trends of the controllers with minimal environmental effects and allowed for experimentation and testing method improvements.

Figure 39. CAVR Test Tank

b. Lake El Estero

Lake El Estero, pictured in Figure 40, located in El Estero Park was the focus of most of the experimental testing and served as the location for decoupled speed and coupled dynamics testing. It is a freshwater lake that is approximately 240 m long and 47–63 m wide and has limited environmental effects other than sea-based wind from the nearby Pacific Ocean and wind-effect waves. It provides a relatively stable testing environment for a small sized USV unable to overcome large environmental disturbances encountered on the open sea.

Figure 40. Lake El Estero, Monterey, California. Adapted from [26].

4. Testing Apparatus and Associated Hardware

The complete testing, pictured in Figures 41–43, for experimental testing included:

1. Lenovo ThinkPad® T460 running Ubuntu Linux OS (ver. 14.04 LTS), MATLAB R2015b with Simulink, and ROS (Distribution Version: Hydro Medusa).

2. Logitech F310 Gamepad USB controller utilized for pre-positioning the KF-USV for trials, launching and recovering the vehicle, and diagnostic testing.

3. CLEARPATH wireless router with antenna and adjustable tripod for extended communications.

Figure 41 is a symbolic representation of the information exchange path of the experimental set up. Figure 42 is a visual overview of the operator's control station and the KF-USV on the lake, which indicates the scale of the test environment for this vessel. Figure 43 and Figure 44 show close up perspectives on individual aspects of the testing apparatus.

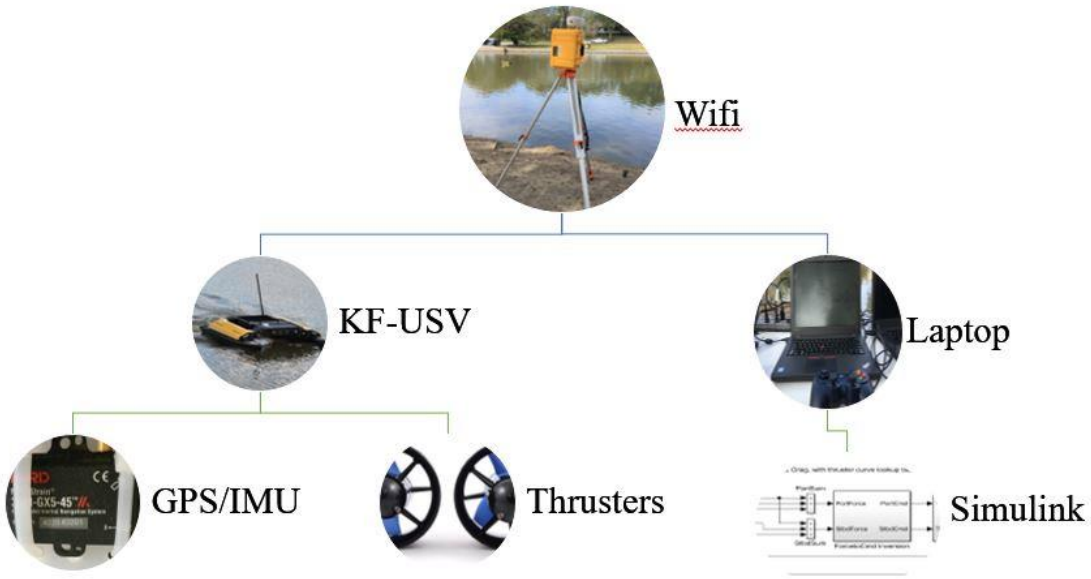

Figure 41. Symbolic Representation of Testing Information Exchange

Figure 42. Lake El Estero Experimental Setup Overview

Figure 43. Lenonvo ThinkPad T460 with Logitech F310 Gamepad USB Controller.

Figure 44. CLEARPATH Wireless Router and Tripod.

5. Environmental Considerations

The CAVR test tank is protected from environmental effects and therefore the cause of error from winds, currents and other factors are considered negligible.

Three days were spent conducting testing at Lake El Estero: 02 February 2018, 14 February 2018 and 28 February 2018. Testing for each day was conducted between 0900–1400 (Pacific Standard Time [PST]) in constant daylight. The weather with regards to temperature (T), wind speed (average and maximum) and precipitation (P) are presented in Table 19 for each experimental session. Best attempts were made to select days of relatively calm conditions to minimize the effect they made have on experimental data.

Table 19. Selected Weather Data from Experimental Testing Days. Source: [27].

Date	**Temperature** (min/max)	**Wind Speed** (avg/max)	**Precipitation** (total)
02/02/2018	10.5 / 23.9 °C 51 / 75 °F	9.6 / 20.9 km/h 6.0 / 13.0 mph	0.0 cm 0.0 in
02/14/2018	7.2 / 15.6 °C 45 / 60 °F	9.6 / 24.1 km/h 6.0 / 15.0 mph	0.0 cm 0.0 in
02/28/2018	10.0 / 14.4 °C 50 / 58 °F	8.1 / 20.9 km/h 5.0 / 13.0 mph	0.0 cm 0.0 in

Underwater currents and other water related environmental factors were not obtained and are unknown. Lake El Estero is a relatively shallow, small and isolated fresh body of water with negligible tidal shifts and therefore environmental effects were not considered as sources of error.

B. EXPERIMENTAL TESTING APPROACH

In contrast to the simulation testing, the experimental testing was limited in time and ability to conduct as rigorous a tuning schedule as during the simulation phase. The experimental testing was limited to coarse tuning using good practices and changes based on visual observation. Analysis in the following sections will focus less on the tuning aspect of the controller techniques and more on the holistic effects of controller techniques on the outcome. As a result, most of the trials compared in the following sections utilize controllers that have been tuned experimentally. In some cases, gain magnitudes vary widely and do not account for tuning iterations.

C. DECOUPLED DYNAMICS

Similar to the simulation testing, the experimental testing was first analyzed the controller design techniques based on decoupled dynamics. Heading control was analyzed initially and speed control was analyzed simultaneously with coupled dynamics during subsequent experiments at Lake El Estero.

1. Heading Control

a. Assumptions and Errors Discussion

The following are assumptions and errors that affected the experimental testing of the heading controller:

1. The KF-USV was assumed to respond to a controller most closely resembling a PD controller for heading control.

2. Based on time and resource constraints, tuning was conducted based on real-time observations of the step response performance and good practice instead of adhering to the tuning table (Table 5) that the simulation testing followed.

3. The chain-fall was a source of experimental error. This chain fall, required for safety, was given enough slack (i.e., loose chain) to allow for the KF-USV to turn freely, in the tank. However, it prevented large translational motion in order to avoid vehicle contact with the sides of the tank. This also resisted the KF-USV's turning motion, which produced oscillatory behavior and prevented the KF-USV from reaching a steady-state. This side effect was unavoidable because the KF-USV turns by forming moments from non-directional water jets, whose motor control units are far more effective at generating thrust in the forward direction than astern. As a result, turning commands inevitably generate a net positive surge motion. This surge motion, and the subsequent oscillations induced by the chain-fall, the settling time and steady-state error will not be utilized as comparison metrics for this set of experiments.

4. Rise time and overshoot proved useful for analyzing the response behavior of the KF-USV, as these metrics were consistent across trial runs. Therefore, these two metrics were used to compare the experimental response of different controllers.

Figure 40 displays an example of multiple runs where the induced oscillation was present in responses around the desired heading set point.

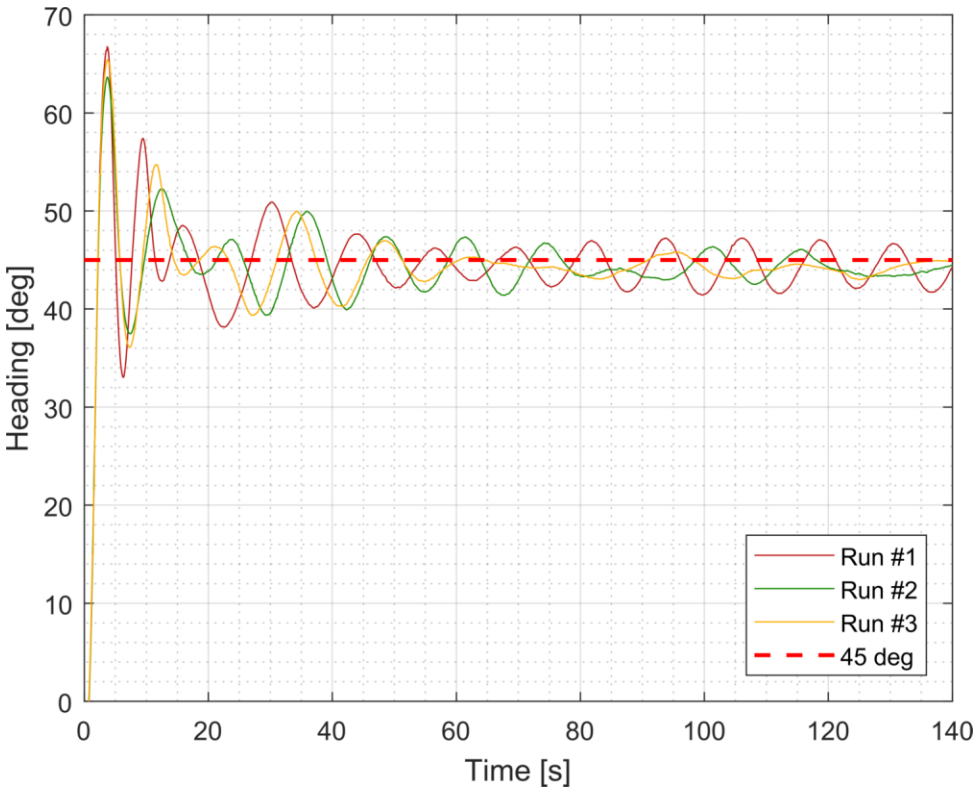

Figure 45. Experimental Heading Control—Oscillation Error Example

b. Linear and Non-Linear Thrust Model Approximations

A series of experiments were conducted in the CAVR test tank to measure the step response to a 45-degree heading command, as described in section III.C.1. First, the linear and non-linear thrust models were coarsely tuned to achieve the desired set-point while minimizing the steady-state oscillations induced by the chain-fall. This error increases proportionally with greater surge speeds, which are correlated to more aggressive turning of the vessel. Therefore, optimal responses for these test cases are not as aggressive as possible (i.e., slower rise time), but they also provide a reasonable experimental comparison. Figure 46 displays four varied responses of the linear (top plot) and non-linear (bottom plot) thrust model approximations that have been coarsely tuned. Table 20 displays

the results of the average performance characteristics. Settling time and steady state error were not discernable and are therefore omitted from Table 20.

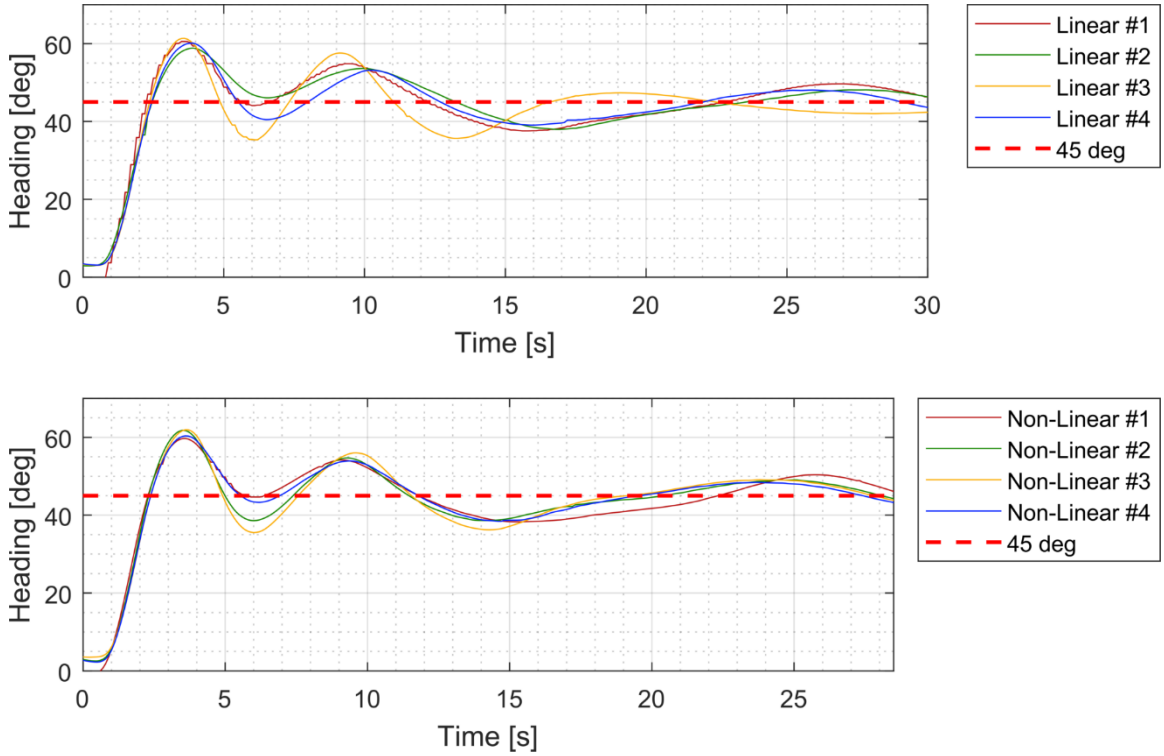

Figure 46. Heading Control—Experimental Step Responses—Linear and Non-Linear Thrust Model Approximations

Table 20. Heading Control—Experimental Results—Performance Characteristics

Thrust Model Selection	Rise Time [s] (Average)	Overshoot [%] (Average)
Linear	1.19	33.82
Nonlinear	1.14	35.43
Difference	0.05	-1.61

From these results, we can make the following conclusions:

1. Despite the oscillations induced by the chain-fall, this captive tank testing was valuable from a developmental perspective. It facilitated system improvements in scripting, sensor integration and controller testing.

2. The responses demonstrate nearly identical behavior and response shape when tuned which correlates to simulation results.

3. The non-linear thrust model performs with more consistency in overall form of the response.

4. The non-linear thrust model has no discernible advantages in step response performance.

2. Speed Control

The basis for decoupled speed control experimentation was identical to the simulation testing (section III.C.2). The objective was to analyze a the closed-loop response to a low-speed (0.0 to 0.25 [m/s]) and high speed (1.25 to 1.50 [m/s]) step command independent of turning dynamics. Each of these experiments were conducted both with and without a feed-forward component, using either a linear or non-linear thrust model approximation. The goal of the experimental testing was to identify the effect of each control technique in a real-world setting.

a. Assumptions and Error Discussions

The following are assumptions and errors that affected the experimental testing of the speed control:

1. Based on the simulation analysis, the KF-USV speed control was assumed to respond best to a PI controller.

2. Based on time and resource constraints, tuning was conducted based on real-time observations of the step response performance and good practice instead of adhering to the tuning table (Table 5) that the simulation testing followed.

3. One source of experimental error was the sensor information provided by the GPS/IMU. Depending on satellite positional information, occasional disruptions in this information stream caused undesired responses from the controller.

4. Step response analysis was complicated based on error in measurements from significant root mean squared (RMS) error in speed measurements at the low set-point.

5. Based on physical constraints of the lake, trial durations for the high-speed runs were limited to prevent colliding with the shore and walls. This limited the analysis of steady-state and settling times in some of the trials.

6. Rise time and overshoot proved useful for analyzing the response behavior of the KF-USV, as these were metrics consistent across trial runs. Therefore, these two metrics were used to compare different controllers. When results permitted, settling time and steady state error are also included in the analysis.

b. Low Speed Control

The low speed control region was tested to compare the impact of different thrust models, as well as the utilization of feed-forward compensation.

(1) Linear versus Non-Linear Thrust Model Comparison

First, the tuned responses for the linear and non-linear thrust models were plotted for comparison in Figure 47. Key performance characteristics are identified in Table 21. These experimental results lead to the following observations:

1. The linear and non-linear thrust models produce nearly identical responses.

2. The non-linear thrust model produces slightly improved performance with regard to rise time, settling time, and percent overshoot.

3. Both responses achieve zero steady state error with little difficulty.

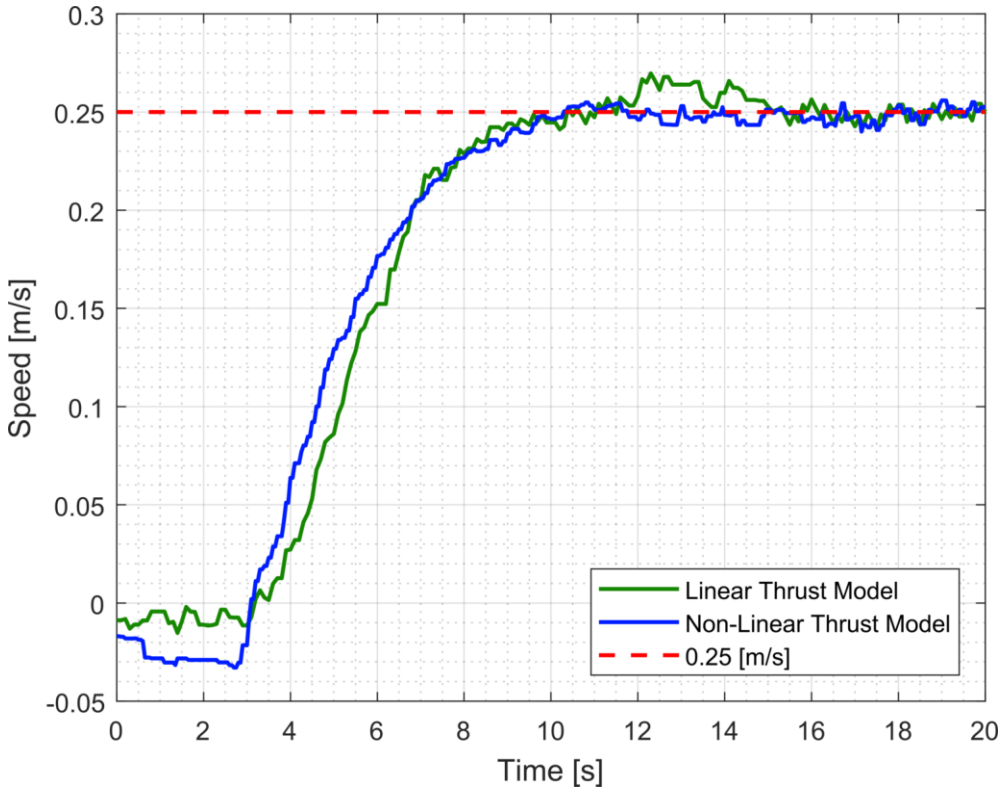

Figure 47. Optimized Experimental Step Responses—Low Speed Control – Linear and Non Linear Thrust Model Approximations

Table 21. Optimized Experimental Performance Characteristics Comparison—Low-Speed Control—Linear and Non-Linear Thrust Model Approximations

Gains		***Rise Time, T_R* [s]**			***Settling Time, T_S* [s]**			***Steady State Error [m/s]***		
Kp (L/NL)	**Ki** (L/NL)	**L**	**NL**	**Δ[s]**	**L**	**NL**	**Δ[s]**	**L**	**NL**	**Δ[m/s]**
24/40	10/15	3.99	4.41	**0.42**	9.11	5.41	**3.70**	0.00	0.00	**0.00**

(2) Feed-Forward Compensation

The step response to speed commands on the KF-USV was tested both with and without the use of a feed-forward term. This term's relationship is identical to the simulation model and expressed by:

$$X_C = \left[16.9|u| + \cancel{X_u}\right]u = 16.9|u|u \tag{11}$$

The basis of comparison for these experiments is the non-linear thrust model approximation. In addition to observing the step-response and accompanying characteristics, the integrator's effort was also recorded to analyze the effect of integrator wind-up, similar to the simulation analysis presented in section III.C.2.a(2). Figure 48 and Table 22 present the results of the tuned response in graphical and tabular form, respectively. From these results we observe the following:

1. The feed forward compensation provides significant improvement in rise time. This can be expected based on its instantaneous thrust contribution, based on set-point, to the motor control unit.

2. The feed forward did over-compensate and produce significant overshoot. This feed forward term was not altered to improve response because it's origination is from experimental testing and model identification and therefore any alterations would be ad hoc and not of any physical importance. Further discussion in conclusions will comment further on the proposed changes to this feed forward term.

3. The integrator for the feed forward compensated system is producing effort to counter the effect of the feed forward. This is opposite to the intended advantage or purpose of including the feed forward term.

Table 22. Optimized Experimental Performance Characteristics—Low-Speed Control—Feed-Forward Compensation

Gains		***Rise Time, T_R* [s]**			***Settling Time, T_S* [s]**			***Steady State Error [m/s]***		
Kp (NF/FF)	**Ki** (NF/FF)	**NF**	**FF**	**Δ[s]**	**NF**	**FF**	**Δ[s]**	**NF**	**FF**	**Δ[m/s]**
40/80	15/25	4.40	0.34	**4.06**	5.41	24.2	**18.79**	0.00	0.00	**0.00**

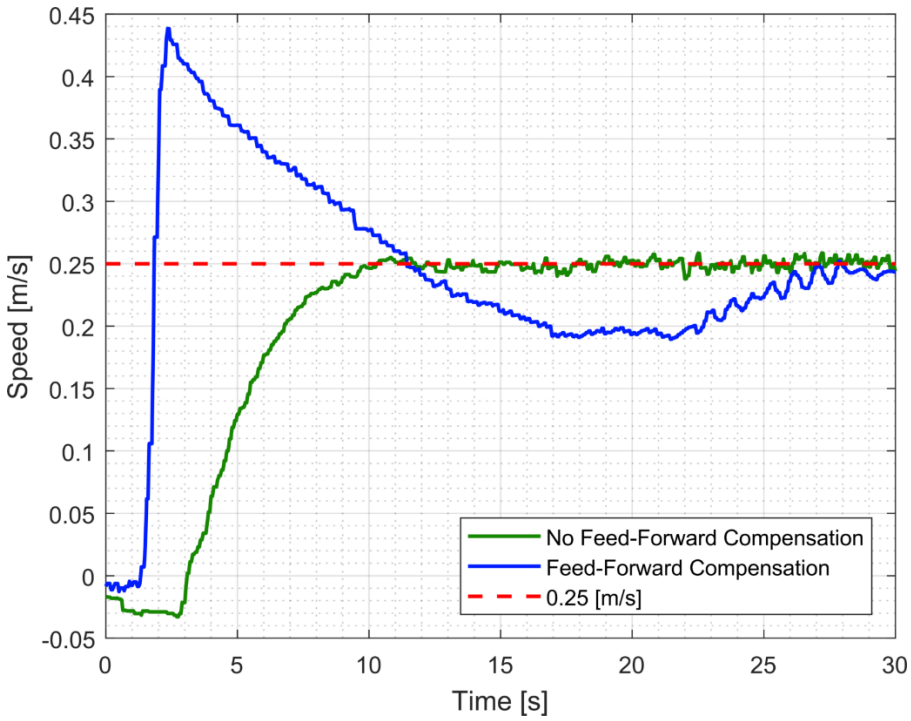

Figure 48. Optimized Step Response—Low-Speed Control—Feed Forward Control

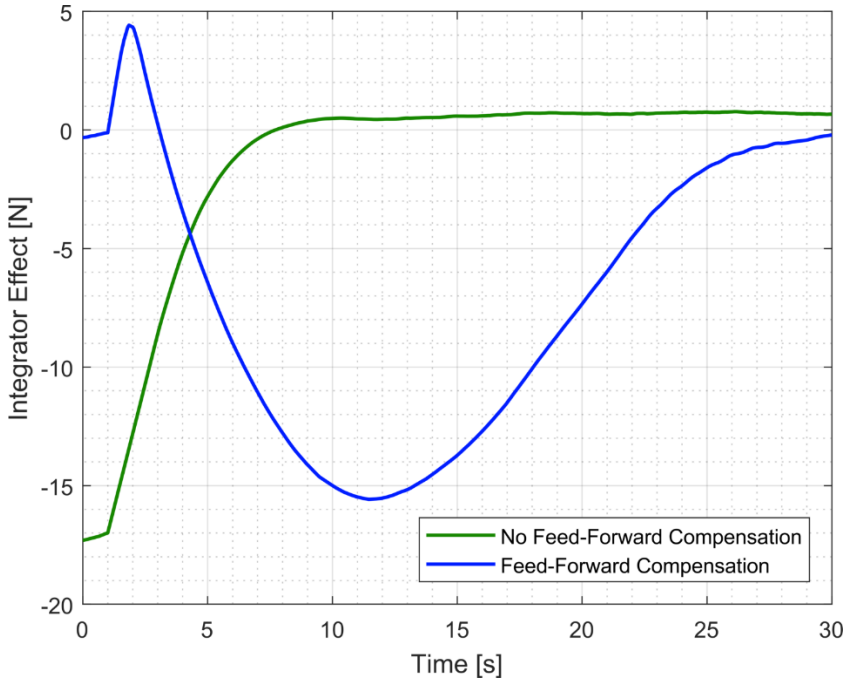

Figure 49. Optimized System Response—Feed-Forward Compensation—Integrator Effort Comparison

c. High Speed Control

The high speed control region was tested to compare the impact of different thrust models, as well as the utilization of feed-forward compensation.

(1) Linear versus Non-Linear Thrust Model Comparison

First, the tuned step responses for the linear and non-linear thrust models were plotted for comparison in Figure 50. Key performance characteristics identified in Table 23. Due to limited number of trials conducted and this speed region for this test case, only two responses are plotted for the non-linear thrust model, and these reflect uncertainty about what might constitute an ideal response. We make the following observations with regards to these step responses:

1. The linear and non-linear models exhibit varied responses, but this may be due to lack of proper tuning for controllers tuned using the non-linear thrust model.

2. All responses trend towards zero steady state error and exhibit similar initial transient behavior.

3. This testing was inconclusive, however, and more trials are required to accurately identify trends in this speed region.

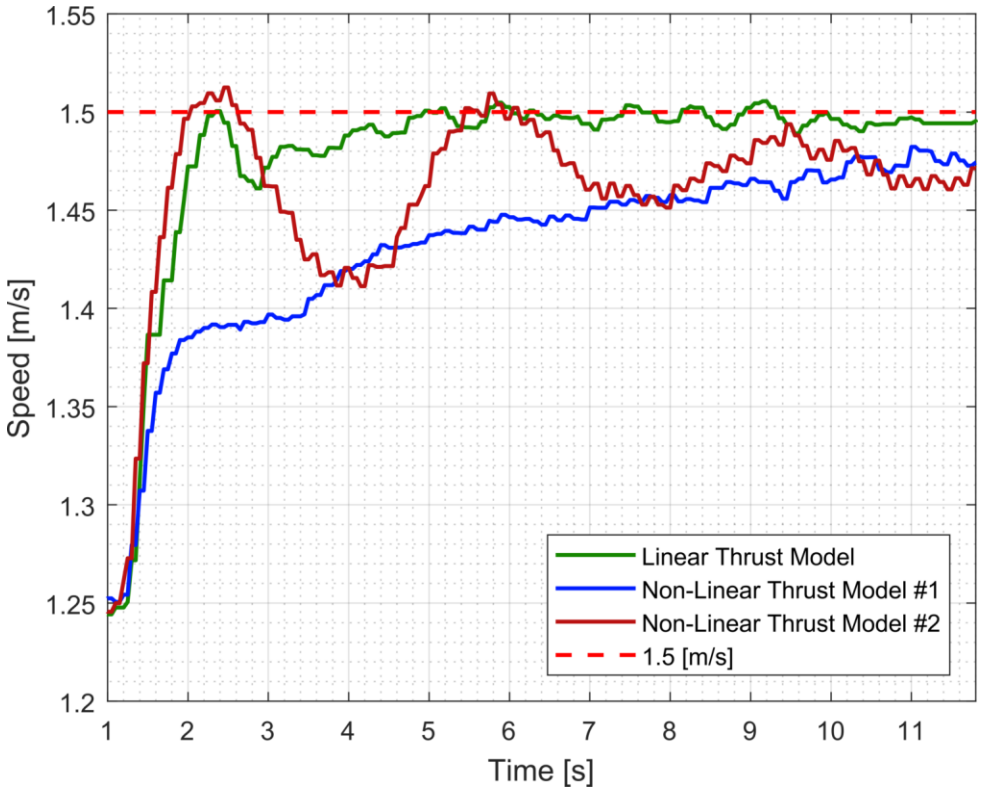

Figure 50. Optimized Experimental Step Responses—High Speed Control – Linear and Non Linear Thrust Model Approximations

Table 23. Optimized Experimental Performance Characteristics Comparison—High-Speed Control—Linear and Non-Linear Thrust Model Approximations

Gains			***Rise Time, T_R* [s]**			***Settling Time, T_S* [s]**			***Overshoot [%]***		
Trial	**Kp**	**Ki**	**L**	**NL**	**Δ[s]**	**L**	**NL**	**Δ[s]**	**L**	**NL**	**Δ[%]**
L / NL #1	40 / 24	15 / 10	0.75	9.82	**9.07**	3.61	10.07	**6.46**	0.00	0.00	**0.00**
L / NL #2	40 / 40	15 / 15	0.75	0.54	**0.21**	3.61	12.12	**8.51**	0.00	1.02	**1.02**

(2) Feed-Forward Compensation

High-speed step responses on the KF-USV was tested both with and without the use of an identical feed-forward term as was used during the low-speed experimentation and simulation phases. The basis of comparison for these experiments is the non-linear thrust model approximation. Figure 51 and Table 24 present the results of the tuned response for each system in graphical and tabular form. A performance comparison similar

to the low-speed test case was conducted. In addition, we also compared the step responses for systems with feed-forward compensation and either a proportional-only (P) or proportional-integral (PI) controller. Figure 52 plots the two responses, one with no integral gain and one with only minimal integral gain to identify trends related to the compensation generated. The effect of the integrators is displayed in Figure 53. From these results we observe the following:

1. As demonstrated in simulation, the tuned feed forward and non-feed forward systems produced similar responses and performance characteristics.

2. Also in common with simulation, the feed-forward term nearly negates the need for the integrator to produce any effort, as indicated in Figure 53.

Table 24. Optimized Experimental Performance Characteristics—High-Speed Control—Feed-Forward Compensation

Gains		***Rise Time, T_R* [s]**			***Settling Time, T_S* [s]**			***Steady State Error [m/s]***		
Kp (NF/FF)	**Ki** (NF/FF)	**NF**	**FF**	**Δ[s]**	**NF**	**FF**	**Δ[s]**	**NF**	**FF**	**Δ[m/s]**
40/80	15/25	4.40	0.34	**4.06**	5.41	24.2	**18.79**	0.00	0.00	**0.00**

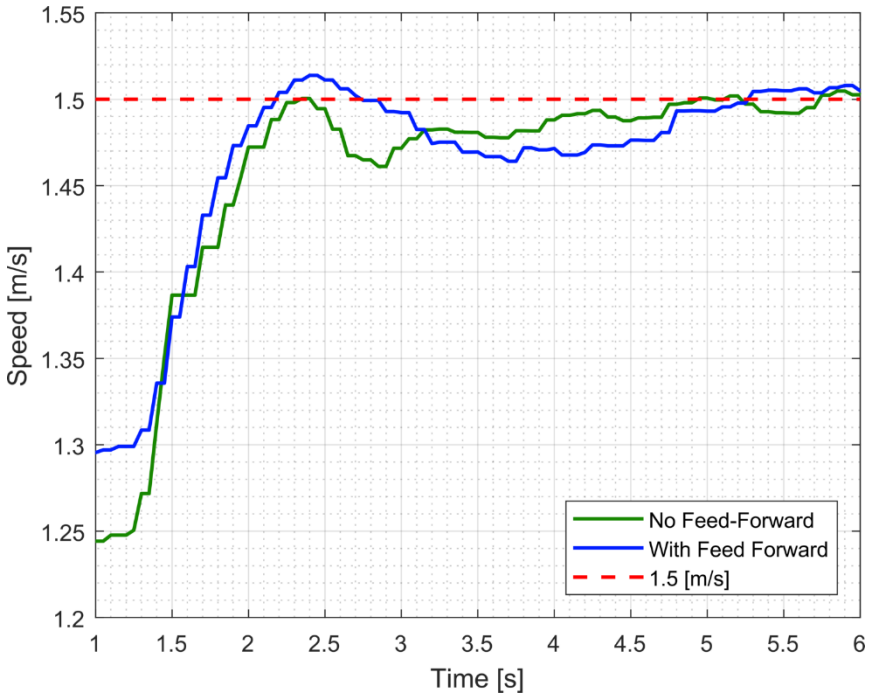

Figure 51. Optimized Step Response—High Speed Control—Feed Forward Control

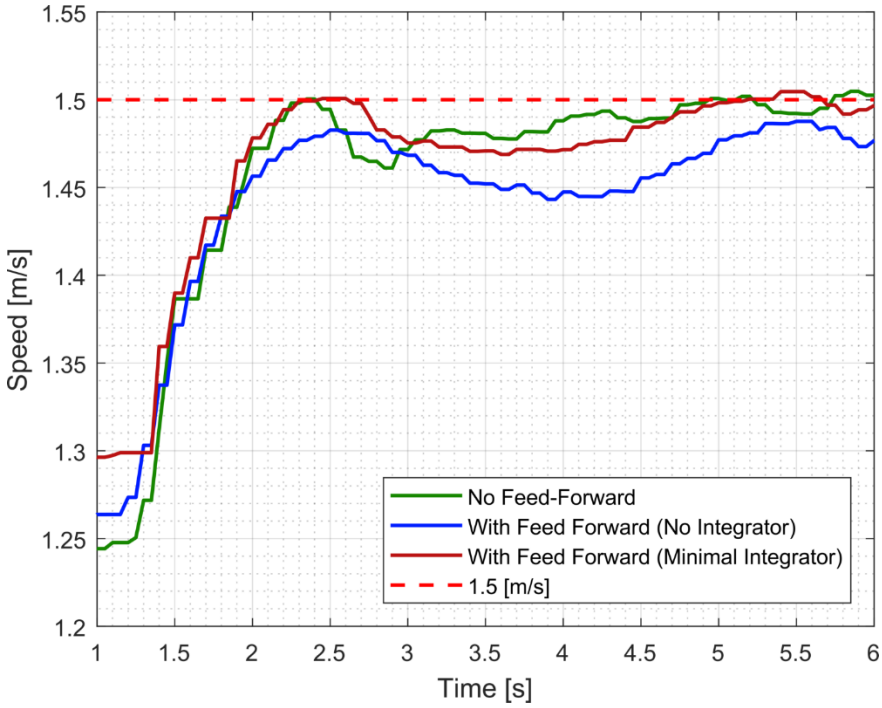

Figure 52. Optimized Experimental Step Responses—High Speed Control—Feed Forward Control Integrator Analysis

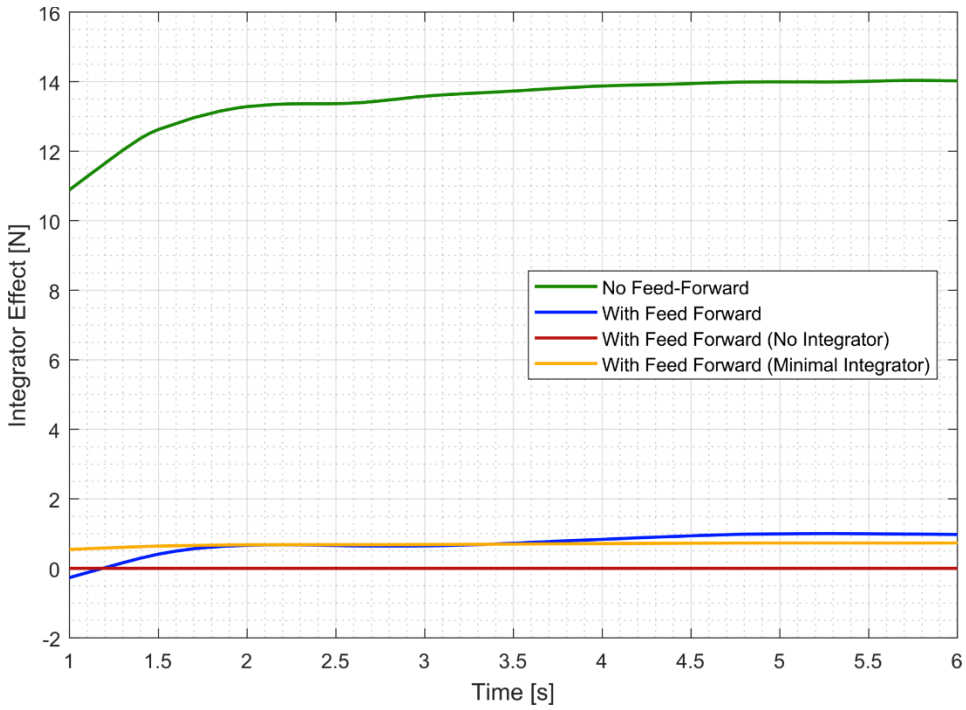

Figure 53. Optimized System Response—Feed-Forward Compensation—Integrator Effort Comparison

D. COUPLED DYNAMICS

To evaluate coupled dynamics, we selected two experimental test cases, commanding a 45-degree turn from steady-state when traveling at: (1) low-speed (0.25 [m/s]), or (2) high-speed (1.25 [m/s]). The systems were tested to analyze the effects of linear and non-linear thrust model approximations, feed forward compensation and combined configurations on heading and speed control performance during the commanded maneuver.

a. Low Speed Turn

The low speed turn was tested to compare different thrust models, as well as the utilization of feed-forward compensation. Figure 54 displays tuned step response for the heading change (top) and subsequent speed response (bottom) of the vessel. Key performance characteristics for heading step responses are identified in Table 25. For this low-speed turning maneuver, we make the following observations:

1. All configurations produce responses that converge to the steady-state value of 45 degrees. They did vary in their transient responses. For example, the linear thrust model with feed forward compensation produced significant overshoot while the linear thrust model without feed forward produced a slower rise time and no overshoot.

2. Heading step commands caused surging in the vehicles speed for all response. The speed controller then worked to the return to the steady state set-point.

3. All responses eventually returned to steady state values for heading and speed respectively.

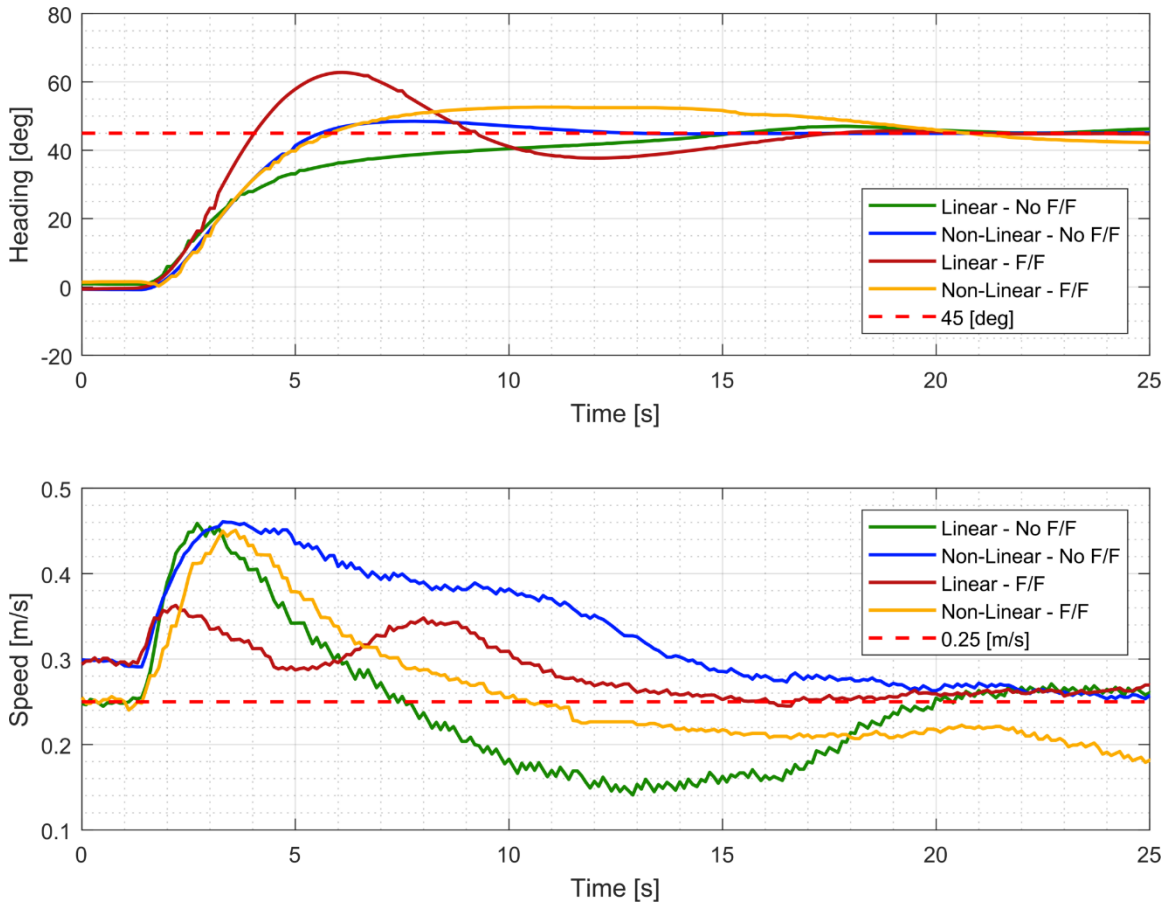

Figure 54. Optimized Experimental System Responses—Low Speed Turn—Coupled Dynamics

Table 25. Optimized Experimental Performance Characteristics Comparison—Coupled Dynamics—Heading Response at Low Speed

Heading Controller Gains			***Rise Time, T_R* [s]**	***Settling Time, T_S* [s]**	***Overshoot [%]***
Case	**Kp**	**Kd**	**L**	**L**	**L**
Linear / No Feed Forward	12.5	5	8.17	13.21	6.79
Non-Linear / No Feed Forward	12.5	5	2.81	11.35	7.78
Linear / Feed Forward	12.5	5	1.81	14.22	39.54
Non Linear Feed Forward	12.5	5	2.71	18.01	16.97

The integrator effect on speed control was recorded and plotted in Figure 55. In contrast to all previous tests, the impact of the feed forward term did not follow the trend of reducing the effect of the integrator. For the linear thrust model, the integrator effect is smaller without the feed-forward term. Conversely, the non-linear thrust model demonstrates the same behavior as previous tests, whereby the integrator effect is reduced by the feed-forward compensation.

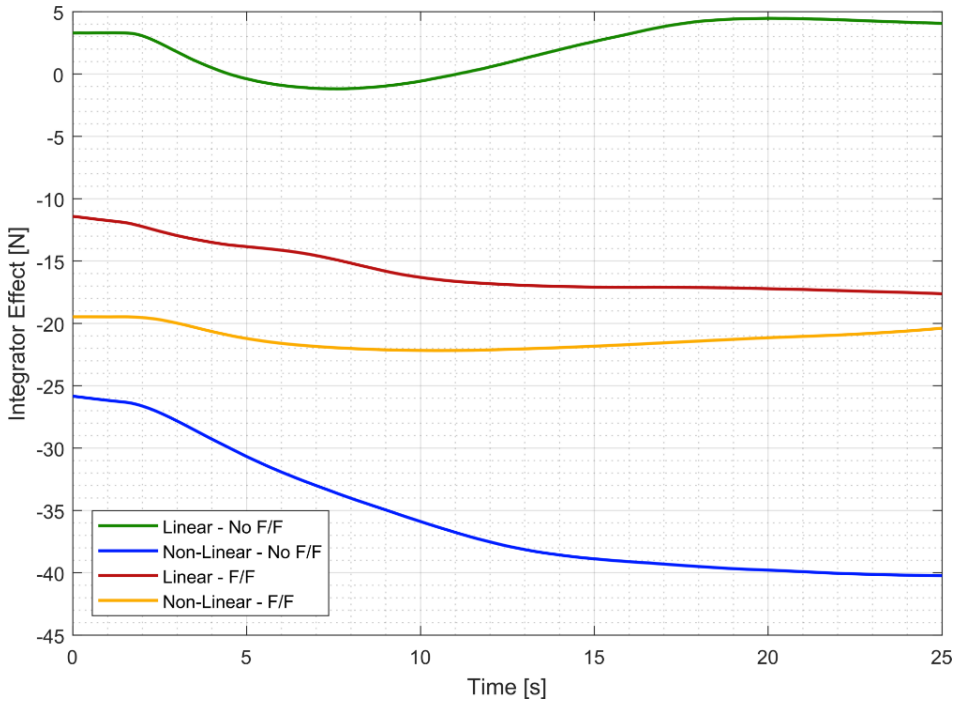

Figure 55. Optimized Experimental System Response—Low Speed Turn—Compensation—Integrator Effort Comparison

b. High Speed Turn

The high speed turn was tested to compare different thrust model, as well as the utilization of feed forward compensation. Figure 56 displays tuned step response for the heading change (top) and subsequent speed response (bottom) of the vessel. Key performance characteristics for heading step responses are identified in Table 26. For this turning maneuver, we make the following observations:

1. All configurations produce very similar responses to the step change in heading.

2. Feed forward compensation decreased rise time and increased overshoot in the system.

3. All responses eventually returned to steady state values for heading and speed respectively.

4. Linear and nonlinear thrust model approximations produced near identical responses.

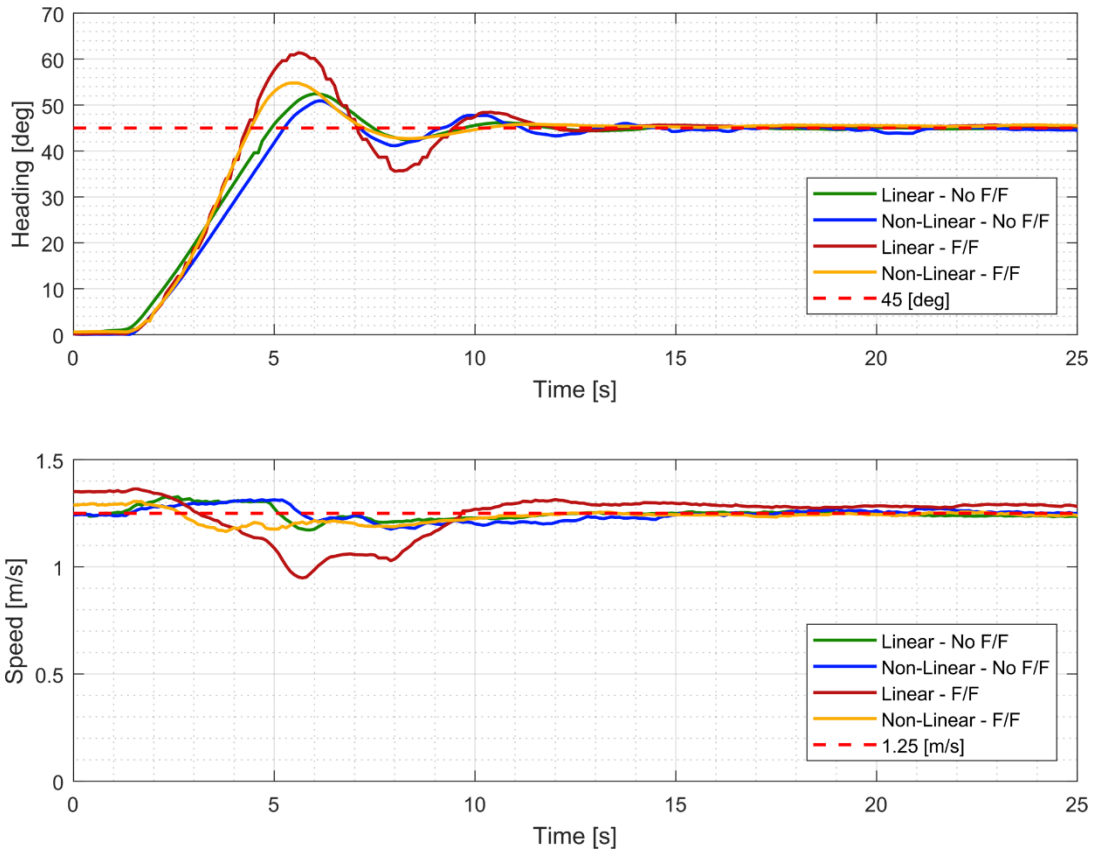

Figure 56. Optimized Experimental System Responses—Low Speed Turn—Coupled Dynamics

Table 26. Optimized Experimental Performance Characteristics Comparison—Coupled Dynamics—Heading Response at Low Speed

Heading Controller Gains			***Rise Time, T_R* [s]**	***Settling Time, T_S* [s]**	***Overshoot [%]***
Case	**Kp**	**Kd**	**L**	**L**	**L**
Linear / No Feed Forward	75	15	2.9071	11.1804	16.5730
Non-Linear / No Feed Forward	75	15	2.9174	11.2301	13.1412
Linear / Feed Forward	100	20	2.1593	11.4816	36.4143
Non Linear Feed Forward	50	12	2.1560	9.6293	21.7687

The integrator effect on speed control was recorded and plotted in Figure 57. The effect of feed-forward compensation followed the consistent trend of reducing the effect of the integrator for a given configuration. When using both the linear thrust model and non-linear thrust model approximations, the integrator effect is decreased when feed forward compensation is included.

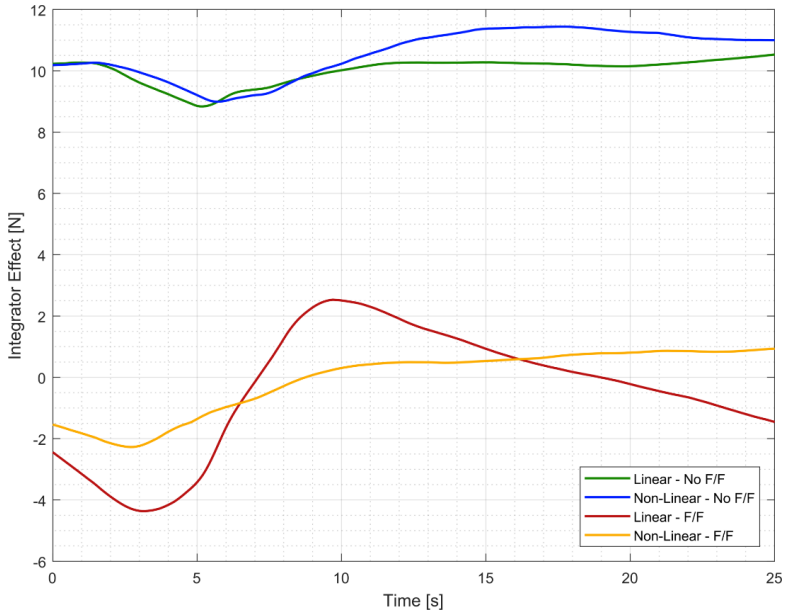

Figure 57. Optimized Experimental System Response—Low Speed Turn—Compensation—Integrator Effort Comparison

E. EXPERIMENTAL SUMMARY

From the experimental testing, we are able to draw conclusions and observations that are critical to the real-world application of these controllers in this specific application:

1. The tuned heading control response was nearly identical for the linear and non-linear thrust model approximations.

2. Speed controllers had difficulty maintaining steady state around the low speed set-point of 0.25 [m/s]. This may be attributed to the following factors:

3. Sensitivity at low speed to external forces and motions generated from environmental factors, e.g., winds and currents, and the resulting disturbance forces.

4. The physical limits of the thrusters to provide smaller and smaller thrust variations to maintain near zero velocity.

5. Velocity measured by the IMU at low speeds can vary greatly and provide inaccurate feedback to the speed controller, which impacts velocity control.

6. Feed forward compensation in the high speed region decreased rise time, but usually increased overshoot for similar tuning requirements.

7. Feed forward compensation also reduced the contribution of the integrator in the speed controller, except when executing a low-speed turn.

8. The system conducted high-speed and low-speed turns efficiently with regards to the heading control.

9. Low-speed turns caused velocity surges, at least partially due to the physics of generating yaw moments with non-directional thrusters instead of control surfaces.

10. High-speed turns produced more efficient speed consistency; a ± 5.7% in speed variance compared to ±27.1% during a low-speed turn. Although, it had the opposite effect of reducing speed during turns, whereas the low-speed experiments increased speed during turns.

Overall, the experimental results provided vital feedback for the implementation of these controllers into the KF-USV. These results facilitated an analysis of controller performance similar to our simulation-based analysis, but these results also included the effects of variable, uncontrollable external forces. The next chapter discusses differences observed between the simulation and experimental results.

V. CONCLUSIONS

The motivation of this research was to use step response performance characteristics to evaluate the extent to which a low-level controller benefits from leveraging improved knowledge of the model to design and tune a small USV's heading and speed controllers. This was done by developing simple decoupled models for speed (surge) and heading (yaw) and implementing a PID controller for feedback control in each degree of freedom. Then, utilizing concepts and theory related to command-compensated control and thruster model selection, several configurations of these PID controllers were developed and tested through simulation and experimentation. Specific configurations investigated were:

1. The use of a feed-forward term (command-compensated) for speed control based on an estimated relationship between commanded steady-state speed and thruster force.

2. The use of an improved non-linear thruster model based on previous experimentation relating thrust force generated by the KF-USV to motor commands. This model was compared against a simple linearized thruster model relationship based on maximum thrust generation over motor command range.

These individual techniques have known effects on similar systems, but this research was conducted in order to investigate the following predictions:

Predictions:

1. The non-linear thrust model approximation will perform with greater consistency with the same controller tuning (i.e., identical gain values) across low and high speed regions, when compared against the linear thrust model approximation. This assumes that the non-linear thrust model is more responsive at these speed extremes, because it more closely resembles the physics of the real-world thruster response.

2. The non-linear thrust model approximation will provide improved heading control response because turning to a precise heading will require the thrusters to respond, during transients, at high and low speeds to generate the necessary yaw moments when called upon.

3. For speed control, feedforward compensation will reduce the need for a large integrator term in the PID controller to achieve steady-state error.

4. By reducing the contribution of the integrator term in the controller, the effect of integrator wind-up is diminished, resulting in faster transient response.

5. Feed forward compensation will improve the baseline step response performance of the speed controller without tuning.

A. COMPARISON OF SIMULATION AND EXPERIMENT RESULTS

The approach of this research involved first establishing a baseline of responses for the decoupled and coupled dynamics equations of motion for the KF-USV in simulation, and then conducting experiments on the actual vehicle for comparison. The following observations highlight differences between simulated and experimental results that are of particular concern for future controller development, and form a basis for later improvements:

1. Simulation-based controllers for speed and heading control, when tuned, resulted in gain constants that are very similar ($\pm 5.8\%$) for both low and high speed test regimes. This implies that one controller can be tuned in one regime, yet still be effective over the entire speed domain. However, the gain constants for controllers implemented in actual experiments varied significantly ($\pm 23.1\%$) when tuned for high and low speed operation. This implies that the experimental controllers could benefit from gain scheduling for effective control. This could be attributed to the inaccuracy of the dynamic model utilized for simulation, as there are other

hydrodynamic forces such as added mass and additional drag terms that effect surge and yaw, and these forces were omitted from our model.

2. Simulated and experimental results varied significantly in the low-speed region where the numerical model does not account for the practical challenges associated with executing low-speed maneuvers against environmental disturbances and inaccurate sensor measurements.

3. Experimental results have significantly slower rise and settling times when compared to simulation, this may be a consequence of such factors as lack of fidelity of the model used in simulation, inaccuracy in estimation of model parameters, or vehicle and environmental effects not captured by the model.

4. There is a lack of quantifiable tuning procedures for comparing controllers in the simulation and experimental domains. The inability to conduct experiments using a consistently robust or methodical tuning procedure, as was conducted in simulation, does not suggest a set of metrics to facilitate comparing the tuning of the controllers over the two domains.

B. CONTROLLER TECHNIQUE BENEFITS ANALYSIS

Despite the differences in the simulation and experimental results, trends in our results nevertheless allowed us to conclude that utilizing model-based knowledge can improve the performance of low-level controllers. Our conclusions based on the original research questions and objectives for this research include:

1. For this particular application, the inclusion of a non-linear thrust model does not result in significant performance improvement. Because significant effort is necessary to develop such a thrust model (either analytically or empirically), this result suggests that neglecting the non-linear thruster characteristics would be a reasonable choice when development time is limited.

2. The utilization of a command-compensated term, in the form of a feed-forward relationship between commanded speed and thruster force, resulted in significant performance improvements. It consistently decreased rise time and was specifically advantageous in the high-speed region of performance. It also provided observable benefits in maintaining speed through the low and high speed turns with coupled dynamics. However, inconsistencies between the simulated and experimental results suggest that the feed forward term may require more accurate model identification or empirical tuning in order to achieve full effectiveness.

3. Qualitatively, the complexity and time spent developing the different control implementations were similar, without significant differences. This suggests that including a feed forward term and non-linear thruster model do not have significant effect on the required development time for these different implementations.

C. FUTURE WORK

Future work for this study would include:

1. Developing a more accurate speed and thrust relationship to increase the benefits achieved from feed forward compensation.

2. Investigating other controller techniques such as L1 or model-reference adaptive controllers (MRAC) and conducting similar comparison studies.

3. Conduct tank testing of the KF-USV and identify hydrodynamic properties and coefficients to improve the representative model of the system. This would likely reduce discrepancies between simulated and experimental controller performance.

LIST OF REFERENCES

[1] J. Katz, "Navy seeks to advance DARPA's sub-tracking USV technology in FY-19," *Inside the Pentagon's Inside the Navy,* vol. 31, no. 9, 2018. [Online]. Available: https://search.proquest.com/docview/2010313127

[2] M. Eckstein, "Navy racing to test, field unmanned maritime vehicles for future ships," *USNI News,* Sep 21, 2017.

[3] Office of Secretary of Defense, "Unmanned systems roadmap (2007-2032)," Department of Defense, Dec 10, 2007.

[4] H. Ashrafiuon, K. R. Muske and L. C. McNinch, "Review of nonlinear tracking and setpoint control approaches for autonomous underactuated marine vehicles," *Proceedings of the 2010 American Control Conference,* 2010. [Online]. https://doi.org/10.1109/ACC.2010.5530450

[5] M. Bibuli *et al.,* "Line following guidance control: Application to the charlie unmanned surface vehicle," *2008 IEEE/RSJ International Conference on Intelligent Robots and Systems,* 2008. [Online]. https://doi.org/10.1109/ IROS.2008.4650890

[6] M. A. Hurban, "Adaptive speed controller for SeaFox autonomous surface vessel." M.S.M.E Thesis, Dept. of Mech. and Aero. Eng., NPS, Monterey, CA, USA, 2012. [Online]. Available: http://hdl.handle.net/10945/6811

[7] S. Kragelund, V. Dobrokhodov, A. Monarrez, M. Hurban and C. Khol, "Adaptive speed control for autonomous surface vessels," *2013 OCEANS,* San Diego, CA, USA, 2013. [Online.] https://doi.org/10.23919/OCEANS.2013.6741115

[8] G. Li, C. Guo, Y. Li and W. Deng, "Fractional-order PID controller of USV course-keeping using hybrid GA-PSO algorithm," *2015 8th International Symposium on Computational Intelligence and Design (ISCID),* 2015. [Online]. https://doi.org/10.1109/ISCID.2015.134

[9] H. Qu, E. I. Sarda, I. R. Bertaska and K. D. von Ellenrieder, "Wind feed-forward control of a USV," *OCEANS 2015—Genova*, 2015. [Online]. https://doi.org/10.1109/OCEANS-Genova.2015.7271438

[10] M. Caccia *et al.,* "Basic navigation, guidance and control of an unmanned surface vehicle," *Auton Robot,* vol. 25, no. 4, pp. 349–365, Nov 2008. [Online]. https://doi.org/10.1007/s10514-008-9100-0

[11] N. S. Nise, *Control Systems Engineering*. Hoboken, NJ, USA: Wiley, 2015.

[12] T. I. Fossen, *Guidance and Control of Ocean Vehicles.* Hoboken, NJ, USA: Wiley, 1994.

[13] T. I. Fossen, *Handbook of Marine Craft Hydrodynamics and Motion Control*. Hoboken, NJ, USA: Wiley, 2011.

[14] "Heron unmanned surface vessel," Clearpath Robotics. Accessed April 13, 2018. [Online]. Available: https://www.clearpathrobotics.com/heron-unmanned-surface-vessel/

[15] Society of Naval Architects and Marine Engineers (U.S.). Technical and Research Committee. Hydrodynamics Subcommittee, "Nomenclature for treating the motion of a submerged body through a fluid: Report of the American towing tank conference," *SNAME Technical and Research Bulletin,* vol. 5, *(1-5),* 1950.

[16] N. Manzini, "USV path planning using potential field model," M.S.M.E Thesis, Dept. of Mech. and Aero. Eng., NPS, Monterey, CA, USA, 2017. [Online]. Available: http://hdl.handle.net/10945/56152

[17] M. Caccia, G. Bruzzone and R. Bono, "Modelling and identification of the Charlie2005 ASC." *14th Mediterranean Conf. on Control and Automation,* 2006. [Online]. https://doi.org/10.1109/MED.2006.328785

[18] K. J. Åström, T. Hägglund and K. J. Åström, *PID Controllers.* Research Triangle Park, N.C, USA. International Society for Measurement and Control, 1995.

[19] R. J. Richards, *Solving Problems in: Control.* Harlow, Essex, England. Longman Scientific & Technical, 1993.

[20] E. O. Doebelin, *Control Systems Principles and Design.* Hoboken, NJ, USA. Wiley, 1985.

[21] D. A. Smallwood and L. L. Whitcomb, "The effect of model accuracy and thruster saturation on tracking performance of model based controllers for underwater robotic vehicles: experimental results," Proceedings 2002 IEEE International Conference on Robotics and Automation, Washington, DC, USA, 2002, pp. 1081–1087. [Online]. https://doi.org/10.1109/ROBOT.2002.1014687

[22] L. L. Whitcomb and D. R. Yoerger, "Development, comparison, and preliminary experimental validation of nonlinear dynamic thruster models," IEEE Journal of Oceanic Engineering, vol. 24, no. 4, pp. 481–494, Oct 1999. [Online]. https://doi.org/10.1109/48.809270

[23] L. L. Whitcomb and D. R. Yoerger, "Preliminary experiments in model-based thruster control for underwater vehicle positioning," in IEEE Journal of Oceanic Engineering, vol. 24, no. 4, pp. 495–506, Oct 1999. [Online]. https://doi.org/10.1109/48.809273

[24] G. Vallabha, Natick, MA, USA. 2016. Real-Time Pacer for Simulink, ver. 1.0.0.1. [Online]. Available: https://www.mathworks.com/matlabcentral/fileexchange/29107-real-time-pacer-for-simulink

[25] B. Bingham, Monterey, CA, USA, 2014. LORD MicroStrain 3DM®-GX5-45 ROS Package. ver 1.1. [Online]. Available: http://wiki.ros.org/microstrain_3dm_gx5_45

[26] "Lake El Estero, Monterey, CA [satellite map]." Google Maps. Accessed May 2018. [Online]. Available: https://www.google.com/maps/@36.5964661,-121.8879305,361m/data=!3m1!1e3.

[27] "Weather History for Monterey, CA." Weather Underground. Accessed May 2018. [Online]. Available: https://www.wunderground.com/history/airport/KMRY/2018/2/28/DailyHistory.html?req_city=Monterey&req_state=CA&req_statename=California&reqdb.zip=93940&reqdb.magic=1&reqdb.wmo=99999

THIS PAGE INTENTIONALLY LEFT BLANK

INITIAL DISTRIBUTION LIST

1. Defense Technical Information Center
   Ft. Belvoir, Virginia

2. Dudley Knox Library
   Naval Postgraduate School
   Monterey, California